DISPERSION AND CHARACTERIZATION OF NICKEL NANOSTRANDS IN THERMOSET AND THERMOPLASTIC POLYMERS

A Thesis

by

CASEY ALLEN WHALEN

Submitted to the Office of Graduate Studies of
Texas A&M University
in partial fulfillment of the requirements for the degree of

MASTER OF SCIENCE

December 2011

Major Subject: Aerospace Engineering

Dispersion and Characterization of Nickel Nanostrands

in Thermoset and Thermoplastic Polymers

DISPERSION AND CHARACTERIZATION OF NICKEL NANOSTRANDS IN THERMOSET AND THERMOPLASTIC POLYMERS

A Thesis

by

CASEY ALLEN WHALEN

Submitted to the Office of Graduate Studies of
Texas A&M University
in partial fulfillment of the requirements for the degree of

MASTER OF SCIENCE

Approved by:

Chair of Committee,	Zoubeida Ounaies
Committee Members,	Ramesh Talreja
	Hung-Jue Sue
Head of Department,	Dimitris Lagoudas

December 2011

Major Subject: Aerospace Engineering

ABSTRACT

Dispersion and Characterization of Nickel Nanostrands
in Thermoset and Thermoplastic Polymers. (December 2011)
Casey Allen Whalen, B.S., Texas A&M University
Chair of Advisory Committee: Dr. Zoubeida Ounaies

Nickel Nanostrands (NiNS) are nano-particles that are highly branched and have a high aspect ratio. These particles show promise as excellent additives to composites when electrical conductivity is desired. Unfortunately, there is very little research done on dispersing powdered NiNS in various polymer matrices. This thesis covers the research in dispersing NiNS in three separate polymer systems, and related composite processing and characterization. An aromatic polyimide (CP2) is first used as a thermoplastic matrix and attempts to incorporate NiNS via an in-situ processing technique concurrent with in-situ polymerization are detailed. Epoxy is then used as a representative thermoset where the NiNS are dispersed in the resin before a hardener is added. The last polymer tested is thermoplastic Polyvinylidene Fluoride (PVDF). NiNS are introduced to this polymer in a solution mixture. Once dispersed, the PVDF solution is heated until the solvent evaporates leaving a PVDF melt containing NiNS, which is subsequently cooled. Samples of all three

polymer nano-composites are created and dispersion is observed with an optical microscope. Using DSC, DMA and dielectric spectroscopy, thermal, mechanical and electrical properties are measured and analyzed.

Results for the CP2 nano-composites showed that during the cure phase, the NiNS settled to the bottom of the films resulting in a non-dispersed composite. This result highlighted the difference between NiNS and other more conventional nano-particles, namely that the NiNS are larger and heavier, therefore are not 'locked into' a dispersed state by the polymer chains. Several techniques were investigated for dispersing NiNS in the epoxy matrix. A method without solvent was shown to be the most effective and resulted in a well-dispersed nano-composite that showed increases in electrical conductivity and dielectric constant as NiNS concentration increases. Enhancement in storage modulus was observed above the composite's T_g as well. PVDF nano-composites also showed good dispersion and a general increase in electrical properties. Below T_g, storage modulus decreases at first before a slight recovery with increasing NiNS. Beyond T_g, the opposite effect is observed. FTIR measurements for the PVDF were also taken and showed no significant changes in the polymer morphology with additions of NINS.

DEDICATION

This thesis is dedicated to my wife. Without her constant love and support, these past few years would not have been quite as wonderful or adventurous.

“A loving heart is the beginning of all knowledge”
- Thomas Carlyle

ACKNOWLEDGEMENTS

I would like to thank my committee chair, Dr. Ounaies for all the opportunities she has given me since I was an undergraduate. I would also like to thank Dr. Talreja and the Aerospace Engineering staff at Texas A&M for making my life easier these past few months so I can focus on this thesis.

I would also like to thank Cameron for their financial support. Without them, this research would not have been possible.

Finally, thanks to my mother and father for their love, support and encouragement and to my wife for her patience, love, cooking and always leaving the light on for me to come home to on those late nights.

NOMENCLATURE

CNF	Carbon Nano-Fiber
SWNT	Single Wall Nano-Tube
TiO_2	Titanium Dioxide
wt%	Concentration by Weight
vol%	Concentration by Volume
NiNS	Nickel Nanostrands
MWNT	Multi-walled Nano-Tube
PVDF	Polyvinylidene Fluoride
CP2	Colorless Polyimide
DMAc	N, N- Dimethylacetamide
PG	Propylene Glycol
6-FDA	6F-Dianhydride
APB-133	1,3' –Bis (3-aminophenoxy) benzene
OM	Optical Microscope
DSC	Differential Scanning Calorimetry
DMA	Dynamic Mechanical Analysis
T_g	Glass Transition Temperature
E'	Storage Modulus
E''	Loss Modulus
δ	Phase Shift Angle

σ’	Conductivity
ε’	Dielectric Constant
FTIR	Fourier Transform Infrared Spectrometry
Pa	Pascal
Hz	Hertz
°C	Degrees Celsius
V_{cry}	Volume Crystallinity
T_m	Melt Temperature
T_{cry}	Crystallization Temperature

TABLE OF CONTENTS

LIST OF FIGURES

LIST OF TABLES

CHAPTER I

INTRODUCTION

1.1 Introduction to composite materials

A composite is a multiphase structure engineered from two or more materials, each displaying different properties. Composites are created in order to achieve a new material that displays a combination of the independent material properties. These unique properties can be combined to alter targeted properties such as electrical conductivity or yield strength. The multiple constituent materials used in the creation of composites are classified as either the matrix or the dispersed phase. The matrix is defined as the constituent material that encompasses and physically supports the dispersed phase, which is added to strengthen or otherwise alter the matrix. An example is concrete, which contains a cement matrix, gravel dispersed phase and sometimes rebar as an additional dispersed phase.

Composites have been of industrial interest for a long time and are steadily advancing in complexity. New materials are constantly required to keep up with the ever-evolving changes in engineering designs and applications. With this rush for more specifically tailored parts, a scientific approach has been taken to the creation of new composite materials. Composites are divided into three general categories: particle reinforced, fiber-reinforced and structural.

_____

This thesis follows the style of *Polymer Journal*.

Structural composites are comprised of sheets with anisotropic properties, which are stacked and orientated depending on the final design specifications. Examples of structural composites include plywood, which has sheets of wood stacked perpendicularly and glued together to negate the effects of directional grain. Fiber-reinforced and particle-reinforced composites both contain smaller constituent materials that are distributed throughout a matrix.

One of the most common fiber-reinforced composites that have been extensively researched and applied is the carbon continuous-fiber reinforced polymer composite [1-3]. Continuous fiber composites are those that have multiple fibers that are unbroken throughout the length or width of the matrix. These composites consist of carbon or glass fibers aligned in one or two directions that are stacked on one another and held in place with a polymer matrix. The carbon fibers used have high strength and relative low weight when bundled with other fibers but are only strong when exposed to tensile stresses. However, a single unidirectional sheet, or lamina, is relatively weak when stressed perpendicularly to the fiber direction, and multiple lamina are therefore stacked as a structural composite to achieve desired anisotropic properties. When the composite is exposed to stress, the matrix material plays an important role by transmitting the stress to the stronger fibers. This allows the composites to resist fracturing or plasticizing at higher stresses than if it were only the pristine matrix material. The matrix can also be selected based on desirable properties such as high temperature functionality or resistance to a specific

environment such as high humidity or acidity. Combined, a stacked fiber reinforced composite can provide a new material that combines the desired properties of both the matrix and the reinforcing component. An issue with structural and long fiber-reinforced composites lies with interfacial delamination and the difficulty to create an isotropic material if needed. Interfacial delamination is a very common mode of failure for these composites and is driven by stresses that occur between layers oriented in different directions. This mode of failure can occur due to the dissimilarity of the matrix and reinforcing components within the composite causing the layers to separate. This problem can be intensified when the composite is exposed to repetitive mechanical stress, temperature changes or even high humidity [2-4].

As an alternative means to increase the physical properties of a matrix material, shorter reinforcement material can be used as opposed to the continuous fibers. Discontinuous, or chopped, carbon or glass filaments can be dispersed in the matrix either aligned in a single direction or randomly oriented. Randomly oriented chopped fiber composites display an isotropic behavior as opposed to continuous or aligned fibers. The disadvantage in this method, however, is a dramatic decrease in the effectiveness of the reinforcing material to strengthen the composite. A majority of the fiber strengthening requires high fiber matrix bond strength to prevent fiber pullout.

The third composite type is particle-reinforced composites. These composites contain small particles that are dispersed into a matrix as a means

to modify their properties. When the particles are in the micrometer range in their size, the composite average properties can be obtained using micromechanics. Often these particles are harder and stiffer than the matrix material and can cause localized movement restraint in the matrix. One use of large particle composites is in modern tires. Carbon black, as small spherical particles, s mixed into a vulcanized rubber matrix. Introducing the carbon black, in this case, is an inexpensive method to increase tensile strength and toughness in the rubber leading to a more durable tire design. Newer forms of composite materials, known as nano-composites, are being heavily researched. The defining difference in nano-composites and large particle-reinforced composites is the size of the particles. Due to the small scale of these particles, the primary interactions between the matrix and dispersed phase are at an atomic or molecular level.

1.2 Nano-composites

A material is considered a nano-composite when the reinforcing constituent is comprised of small particles, or fillers, with a dimension of 100 nm or less. A common matrix material used for nano-composites is polymer. There has been plenty of research on nano-composites consisting of nano-fillers such as Carbon Nano-Fibers (CNFs), Single Wall Nano-Tubes (SWNTs) and Titanium Dioxide (TiO_2) [5-13]. These new composites interact with the matrix material at a molecular scale and can be tailored to create a new material while still largely

maintaining the apparent homogeneity of the matrix material. Given the size of the nano-fillers, a nano-composite could have isotropic properties if needed; in addition, nano-filler/polymer interface can be tailored to result in molecular level interactions. One common use of these new nano-composites is turning an insulating polymer into an electrically or thermally conductive material without negatively impacting the mechanical properties [6-8]. An oft-cited example of the need to alter a material's electrical properties would be for lightning strike mitigation in aircraft components. This can be done by integrating a conductive nano-filler particle into a naturally insulating matrix thereby creating a conductive pathway through the material without detrimentally impacting the mechanical or thermal properties [13]. Another potential use could be to more evenly distribute temperature to prevent thermal degradation at a localized spot due to temperature gradients [12].

One of the biggest challenges faced in the processing of nano-composites is to break up agglomerations of the nano-filler into individual strands and then evenly disperse these particles throughout the matrix [14-17]. Agglomerations occur when the nano-particles are grouped in a bundle due to their large surface to volume ration and the dominating van der Waals forces at the molecular scale. If agglomerations cannot be overcome then a much larger weight percentage (wt%) of the filler must be used to achieve the desired electrical or thermal enhancements often at a cost to other properties [18]. Agglomerations could also physically weaken a composite by becoming a stress

concentration point. A micrograph showing an agglomeration of multi-walled nano-tubes (MWNTs) in a polymer matrix is displayed in Figure 1-A.

Along with breaking down agglomerations, the particles in a nano-composite must also be well dispersed throughout the matrix. If homogenous distribution is not achieved, it can essentially lead to a two-phase composite where one phase is particle rich and the other is relatively particle free. These two-phase composites are unpredictable in nature and cannot be used reliantly for any manufacturing processes. An early attempt at dispersion of high wt% Nickel Nanostrands (NiNS) in this thesis research is shown in Figure 1-B revealing a two-phase composite. The black regions are where high concentrations of NiNS reside while the yellow-orange areas have a dramatically smaller percentage of this filler material appearing almost as pristine polymer. A large part of this thesis research topic focuses on overcoming agglomerates and creating a well dispersed nano-composite between nano-sized filler material and various polymer matrixes.

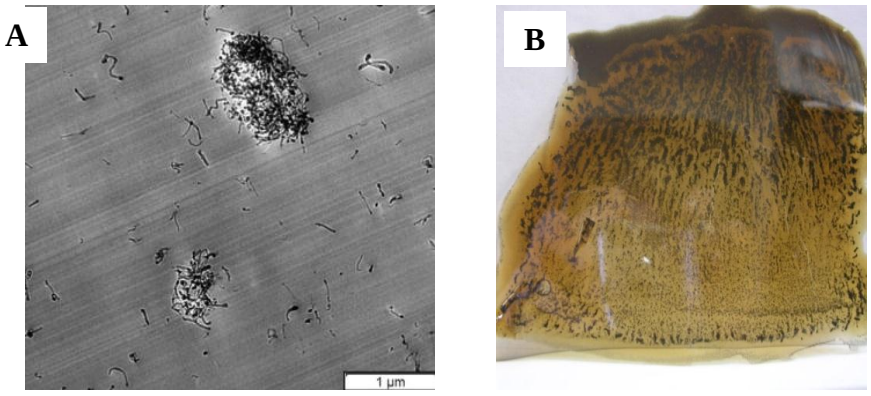

Figure 1: (A) Agglomeration of MWNT [18] (B) Two phase composite

There have been multiple techniques to aid in the dispersion of nano-fillers including the use of surfactants, sonication and functionalization of the fillers and other novel processes [19-26]. Functionalized fillers are created when a chemical functional group is attached onto the filler before the processing stage of the composite. These functionalized side groups serve to modify the surface of the fillers to increase interaction between the particles and the matrix. Surfactants on the other hand work to increase dispersion by reducing the surface tension of a liquid or the interfacial tension between two materials. Sonication works by creating rapid vibrations in a medium causing violent formations and collapses of microscopic bubbles that physically separate and disperse the nano-scale particles. This technique will be the primary tool used to aid in dispersion throughout this research.

1.3 Nickel nano-strand particles

CNFs, SWNTs, TiO_2 and other nano-scale fillers have largely been studied and characterized in a variety of different matrix materials [5-9, 12, 27, 28]. Nickel Nanostrands, however, are relatively new and have not been studied to such an extent. Nickel Nanostrands are often compared to SWNTs based on their high aspect ratio and nanometer sized diameters [11]. Differentiating the two is that NiNS have a unique 3D geometry in that they are highly branched and interconnected [10, 11]. NiNS also have the properties commonly associated with nickel, such as high electrical conductivity, electromagnetism

and high chemical resistivity [11]. Due to their unique geometry and high electrical properties, NiNS should easily create a highly conductive nano-composite since the branches of a NiNS are more likely to encounter other particles than narrow and straight SWNTs. A large driving factor for any new material however, is price versus effectiveness. Pristine SWNTs are sold for approximately $200 per gram whereas NiNS can be purchased in bulk averaging near $5 per gram. This price difference can be a large factor in the fabrication of a new material in industry even if a larger quantity of NiNS is required to achieve the same effects as SWNTs.

Most research pertaining to NiNS have focused on using them either in conjunction with CNFs or as a single layer on the surface or between two materials [10, 11, 27-31]. Placing a highly concentrated layer of NiNS on the surface of a material allows for a conductive path along the outside without greatly influencing weight. However, in some applications, there may be a need for a bulk thermal or electrical conduction. In that case, the NiNS would have to be added during the processing phase of the material to form a network in the matrix itself. Research involving NiNS and CNF place a heavy emphasis on the conductivity and dispersion of the CNF. Very little research has been done on dispersing only NiNS in a polymer mixture [11, 29, 32]. By focusing on NiNS nano-composites, this project fills a gap in knowledge and facilitates exploiting the unique 3D geometry of NiNS.

1.4 Polymer matrix

Most literature showing NiNS dispersion in a polymer matrix deal with cases that are only processed via shear mixing and are cast by injection molding or other rapid cooling processes effectively locking the NiNS in the matrix [11, 29, 31, 32]. However, these methods require a large concentration of NiNS to produce a conductive composite and limit the type of polymers that can be used [11, 29, 31, 32]. Polymers can be generally divided into two categories: thermoplastics and thermosets. Thermoplastics are polymers that, once formed, can be reheated to a point where they are melted and can be reformed into a different shape. The melt can then be cooled and hardened into a new product completely independent of the previous history. Thermosets cannot be melted once cured, rather, when taken to a high enough temperature, the polymer begins to first harden, then degrade and finally chemically break down. Due to these differences, both types of polymers are processed as matrices. The polymers that will be studied in this research include an Air Force grade epoxy, Polyvinylidene Fluoride (PVDF), and an aromatic colorless polyimide (CP2). The epoxy is a thermoset and is processed using a resin and a curing agent. The PVDF and CP2 are both thermoplastics; the PVDF will be processed as a melt while the CP2 will undergo in-situ polymerization. During in-situ processing, the polymer chains form and encompass nano-particles reducing movement and ideally creating a well-dispersed composite.

1.5 Problem statement

The objective of this thesis research is two-fold: 1) to create several Nickel Nanostrands-reinforced nano-composites that show good optical dispersion and 2) to investigate resulting changes in mechanical, thermal, electrical and dielectric properties. To accomplish the first objective, polymers with different processing techniques are used as the matrix material to determine which processes can successfully disperse NiNS as well as retain the dispersion during its cure cycle or solidification. Building upon previous experience in nano-filler dispersion in thermoplastics and thermosets, the focus of this thesis will be on dispersing the NiNS in model polymers as individually dispersed strands or as small nano-scale bundles. An attempt to disperse NiNS via an in-situ processing technique will also be examined and attempted. The second objective will be to examine any changes in basic material properties dependent on the concentration of NiNS present in the polymer matrix. The results will then be compared and discussed to determine the effectiveness of the various processing techniques.

CHAPTER II

EXPERIMENTAL

2.1 Materials

In this chapter, the filler material to be dispersed is discussed as well as the solvents DMAc and Propylene Glycol, which aid in dispersing the NiNS as well as dissolving the polymers. The polymers that are being investigated include a colorless aromatic polyimide, epoxy and PVDF. Each item is used as received without undergoing any additional modifications not mentioned in this thesis.

2.1.1 N, N- Dimethylacetamide

One common solvent used in this research is N, N- Dimethylacetamide (DMAc). The chemical structure of DMAc is shown in Figure 2. DMAc is a polar solvent and was chosen due to its ability to dissolve the polymers under study and due to its possible affinity to metal nano-particles. DMAc was heavily used in previous dispersion studies and showed success in dispersing SWNTs.

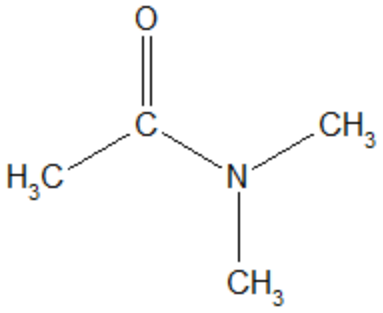

Figure 2: Molecular Structure of Dimethylacetamide

2.1.2 Propylene glycol

Propylene Glycol (PG) was considered as a possible alternative to DMAc due to its reported interaction with nickel particles[19]. Various solvents were tested alongside DMAc for their interaction with NiNS including dimethylformamide, water, methanol, acetone, PG, tetrahydrofuran and toluene. It was determined that PG was the only solvent that outperformed DMAc and was therefore pursued. NiNS are probe-sonicated in Propylene Glycol for 15 minutes to disperse the NiNS. Figure 3 shows the PG molecular structure.

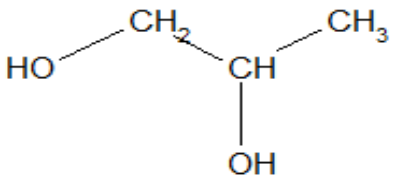

Figure 3: Molecular Structure of Propylene Glycol

2.1.3 Nickel nano-strands

The NiNS used in this work were provided by Conductive Composites Company through Cameron. With a reported 99.999% purity, these NiNS have a density of 8.92 g/cm^3, a diameter from 50 nm to 2µm and an aspect ratio ranging from 50:1 to 500:1 [11]. This diameter is much larger than the oft-compared CNFs as well as having a significantly smaller aspect ratio. Due to this increased diameter and shorter aspect ratio, it may prove difficult to disperse when using common nano-composite processing techniques. Figure 4 contains images

obtained from the Conductive Composites online media gallery. It can be seen that while some strands are large in comparison, there are a few branches with a very small diameter on the same particle leading to largely varying diameters throughout each particle. NiNS are also weaker than CNFs and when placed under extreme duress may split and fracture which could effectively eliminate any gain presented with its 3-D geometry. However, too little force to the NiNS may cause a non-dispersed nano-composite full of undesirable agglomerations that may hinder achieving optimal properties. The 3-D geometry has advantages in terms of achieving a percolating network but it also poses challenges in terms of ensuring polymer infiltration and wetting during processing.

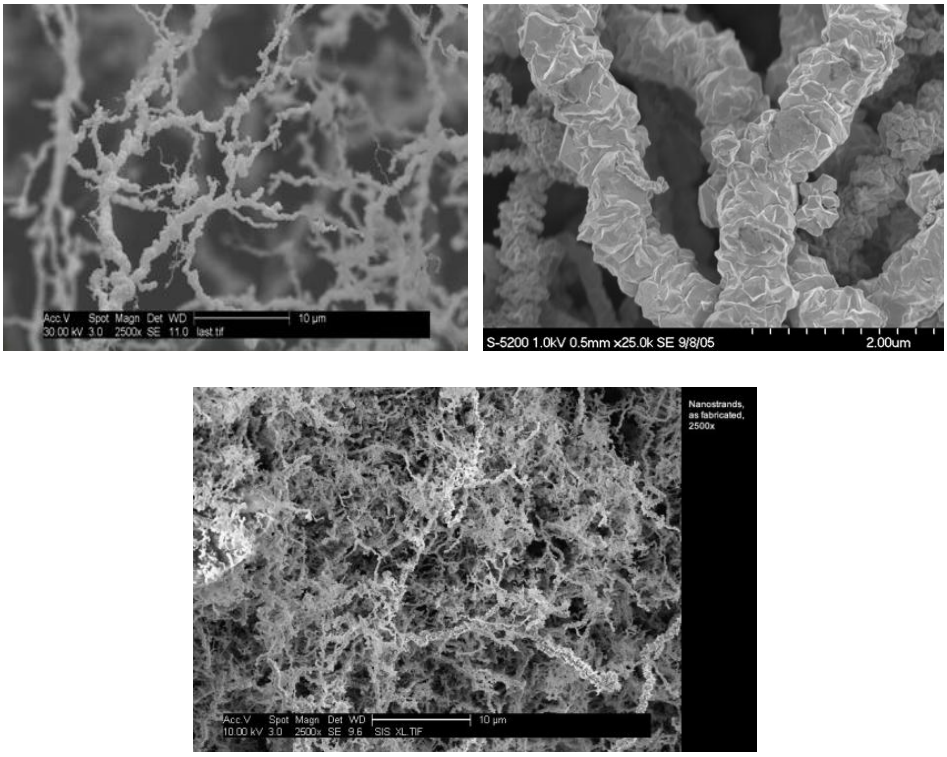

Figure 4: NiNS images provided by Conductive Composites online gallery

2.1.4 Aromatic colorless polyimide

The aromatic colorless polyimide (CP2) was considered as a polymer matrix for NiNS due to our previous experience with in-situ processing with Single Wall Nanotubes (SWNTs)[7]. This thermoplastic polymer is created by combining two monomers, 6F-Dianhydride (6-FDA) and 1,3'-Bis (3-aminophenoxy) benzene (APB-133) at a 10 – 6.58 gram weight ratio respectively. Molecular structures of both powders and the resultant polyimide are shown below in Figure 5.

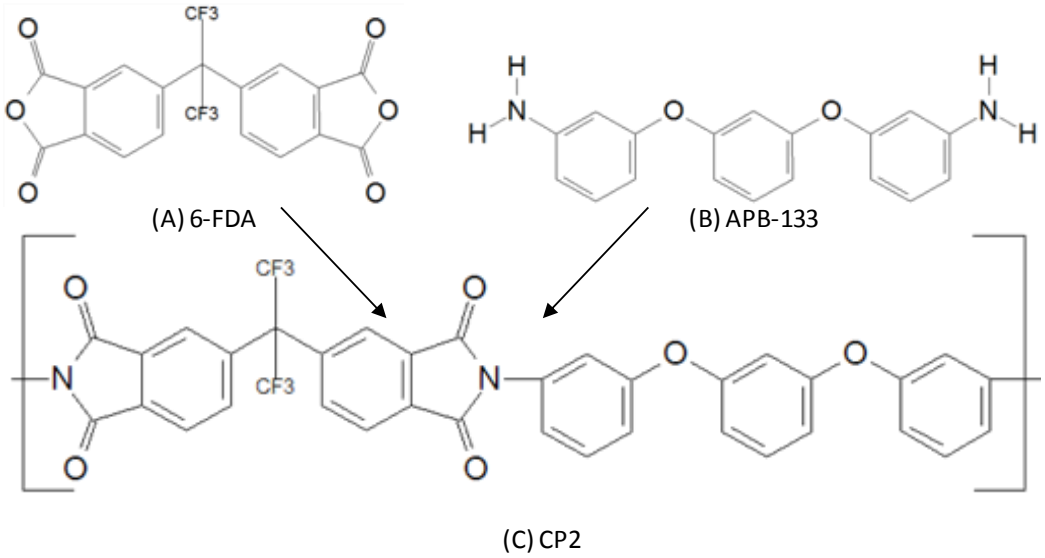

Figure 5: CP2 Polyimide configuration (A) 6-FDA (B) APB-133 (C) CP2

2.1.5 Epoxy

The thermoset epoxy used in this study is composed of a resin and a curing agent. The Epon™ Resin 862 is a liquid epoxy resin with low viscosity.

Epikure W is a non-mda aromatic amine curing agent with low viscosity, very long working times and provides high performance properties once cured. Both chemicals were purchased from Miller Stephenson. Figure 6 displays the chemical structures for Epon 862 and curing agent W, which are mixed in a 100 – 26.4-gram weight ratio respectively. Once combined, the curing agent and resin begin to crosslink to form the hardened epoxy. The mixture can be cured with different heat profiles often using 177°C as the final cure temperature.

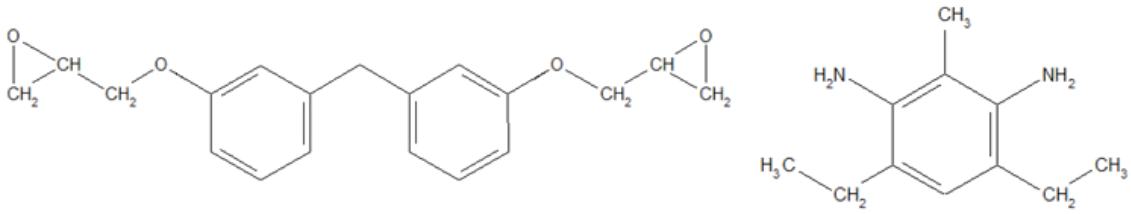

Figure 6: (A) Epon 862 Resin (B) Epikure W Curing Agent

2.1.6 Polyvinylidene fluoride

Polyvinylidene Fluoride (PVDF) is a thermoplastic fluoropolymer, which is morphotropic, where three of the possible crystal structures can be polar. PVDF was purchased from Arkema as a fine milled powder under the name Kynar 301-F. The melting point of this thermoplastic is listed as between 155 and 165˚C and is easily dissolved in DMAc. The simple chemical structure of PVDF is shows in Figure 7.

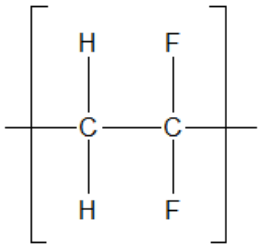

Figure 7: A repeat unit of a PVDF polymer chain

2.2 Processing equipment

To disperse NiNS into a polymer matrix, several instruments were available during the particle dispersion and polymer processing. One useful tool in the dispersion of nano-sized particles is the Model 100 Sonic Dismembrator, or probe sonicator. The probe sonicator works by transforming an electrical alternating current into mechanical motion by a piezoelectric transducer. The tip of the probe begins to vibrate quickly causing the creation and destructive collapse of micro-bubbles. On a larger scale, when these bubbles collapse, a large amount of energy is released at a high intensity. This energy disrupts intermolecular interactions and scatters particles present in a solution in an attempt to create a well-dispersed solution. Placing the probe sonicator tip directly into the solution is a method known as direct sonication. A Cole-Parmer® stainless steel ultrasonic cleaner, or bath sonicator is used to help disperse particles when direct sonication is not desired. Indirect sonication with this method results in a lower intensity mixing but allows for sonication when the particles are dispersed in a more viscous solution that may damage a probe

sonicator tip. The bath sonicator also allows the solution to be heated up to 69°C and be mechanically mixed while still undergoing sonication.

To aid in physically dispersing particles in a more viscous solution, an IKA® RW 20 Digital Dual-Range Mixer, mechanical or shear mixer is used with a propeller blade attachment. With adjustable speeds, this shear mixer allows for uniform distribution of particles and can physically separate agglomerates by shear force. With a powerful motor, this shear mixer ensures that a constant RPM is achieved throughout a wide viscosity range. To heat a solution above 70 °C, a Corning PC-6200, or hot plate, is used. Magnetic stirring is an option with this instrument but not useful due to the NiNS being attracted to the magnetic stirrer. The hot plate has a temperature range from room temperature to 550°C, which allows for thermal control over a polymer, such as creating a melt or lowering the viscosity. As an open surface, the hot plate can be used in conjunction with the shear mixer to help control viscosity or to evaporate a solvent. Polymer curing or solvent evaporation are achieved by a Ney 2-160 Kiln (2-stage oven). This enclosed environment can be purged with nitrogen gas to prevent oxidation at higher temperatures for certain polymers such as CP2.

2.3 Processing of NiNS-polymer nano-composites

Several processes are used in an attempt to disperse Nickel Nanostrands in a thermoset epoxy and various thermoplastics. This section is dedicated to describing, in detail, the processes used to create these nano-composites.

2.3.1 CP2 composite processing with DMAc solvent

The NiNS were first probe sonicated for 5 minutes in DMAc. A tri-neck flask was purged with N_2 and this purge was maintained for the entire processing procedure. After successfully dispersing the NiNS, they are then added to the 6-FDA powder in the tri-neck flask. This solution was mechanically sheared and bath sonicated for 30 minutes at which point the APB-133 powder was added. Bath sonication and mechanical shearing were continued for 3 hours followed by 21 hours of only mechanical shearing all while still under a N_2 atmosphere. At the end of this step, some of the viscous solution was poured onto a glass plate and spread into a thin film with a doctor blade at a desired thickness. The film was then cured in a N_2-purged oven. Figure 8 is a flowchart illustrating the processing of NiNS – CP2 composites.

2.3.2 Epoxy composite processing with DMAc solvent

Epon 862 is the model thermoplastic considered in this project. Unlike thermoplastics, such as CP2, epoxy will harden during curing due to crosslinking. Solvent based processing was pursued first. In this technique, the NiNS are first dispersed in a DMAc solvent using probe sonication. The optimal amount of time for good dispersion without causing damage to the NiNS structure was studied and determined to be between 5 to 15 minutes. Due to the fact that the following steps included bath sonication, the solution was only exposed to 5 minutes of probe sonication in an attempt to limit NiNS breakage.

This solution was placed in a beaker with the EPON resin 862 and then sonicated for an hour in the ultrasonic bath and mechanically sheared at 300 RPMs.

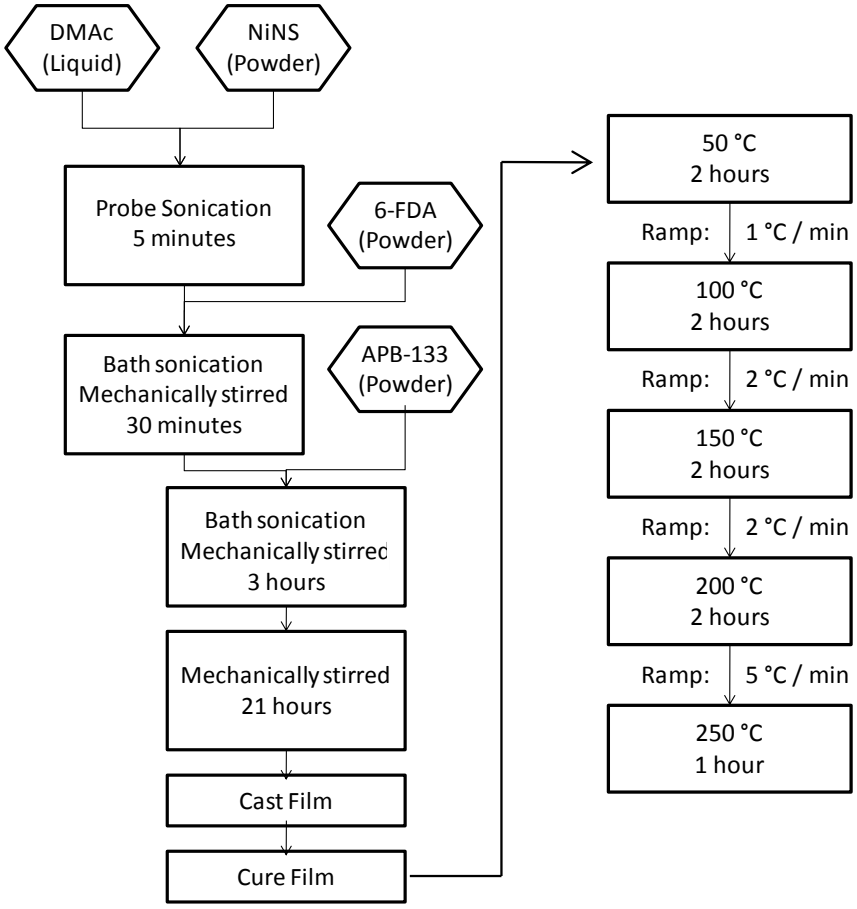

Figure 8: CP2 processing chart

After an hour of sonication and shear mixing, the solution was placed in a vacuum oven at 80˚C under vacuum until the DMAc was fully evaporated as determined by weight change. EPIKURE W curing agent is then added to make

a 20g mixture that is again sonicated and mechanically sheared at 300 RPMs for 1 hour. The mixture is then placed back in the vacuum oven momentarily to remove any trapped gasses. The mixture is then poured into a mold coated in a high temperature heat release agent and cured in an oven for two hours at 125˚C followed by two more hours at 177˚C. Figure 9 displays the processing used to create a solvent-based NiNS – Epoxy composite.

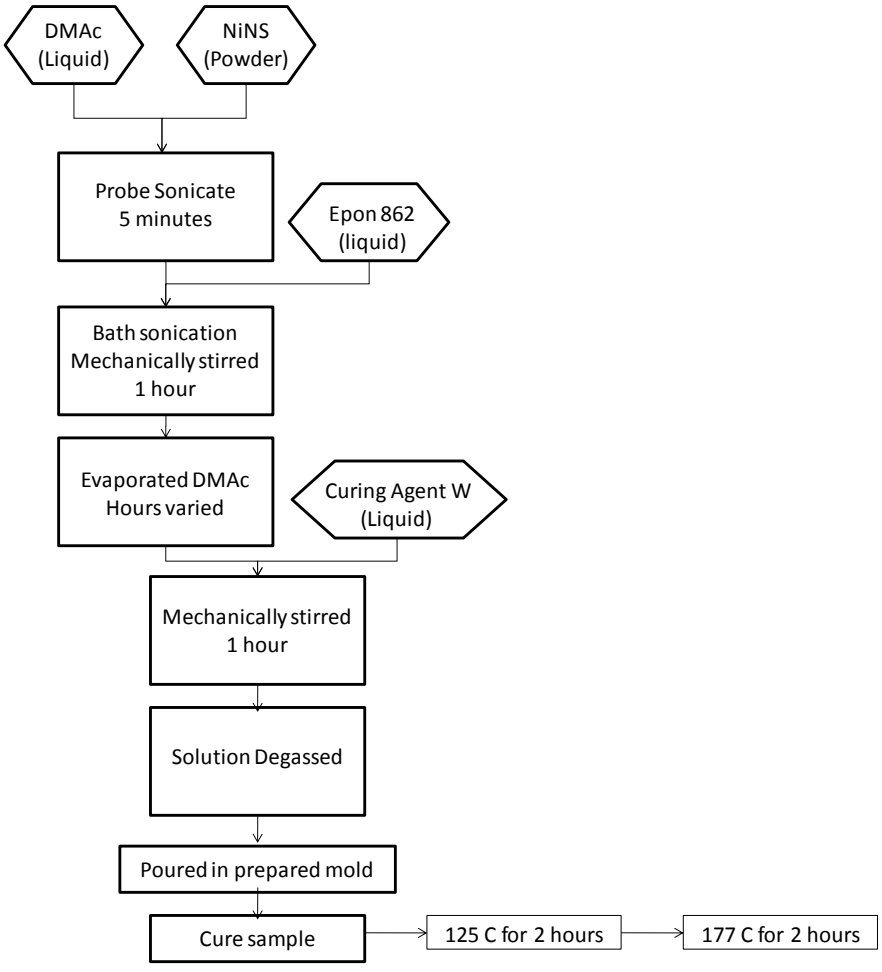

Figure 9: Solvent based NiNS – Epoxy processing chart

The hardened epoxy composite was removed from the mold and the NiNS dispersion was observed using the optical microscope. A representation of the dispersion through the thickness was obtained by focusing the microscope at different levels starting from the top layer and moving to bottom layer with identical step sizes. The top layer refers to the surface exposed to atmosphere during the cure cycle and appears glossy whereas the bottom layer is in contact with the mold and appears dull. If dispersion is visually seen, the composite is then cut into the appropriate sample size using the saw while surface voids and defects are removed using the polisher. The samples are then characterized with the DSC, three-point bending in DMA and the Dielectric Spectrometer.

Figure 10 (A) is a picture of an epoxy sample cured in its mold with the top side visible; (B) is the mold after epoxy removal; (C) and (D) show the top side of the sample and displays the glossiness of the surface. The top side of the sample is the surface through which OMs are taken from. Figure 10 (E) and (F) show the bottom side of the sample and reveals how this surface is not glossy as well as showing some voids and surface defects. The OM is not able to focus beyond the surface layer when viewed from the bottom layer possibly due to the heat release agent used to insure easy removal of the epoxy sample once cured.

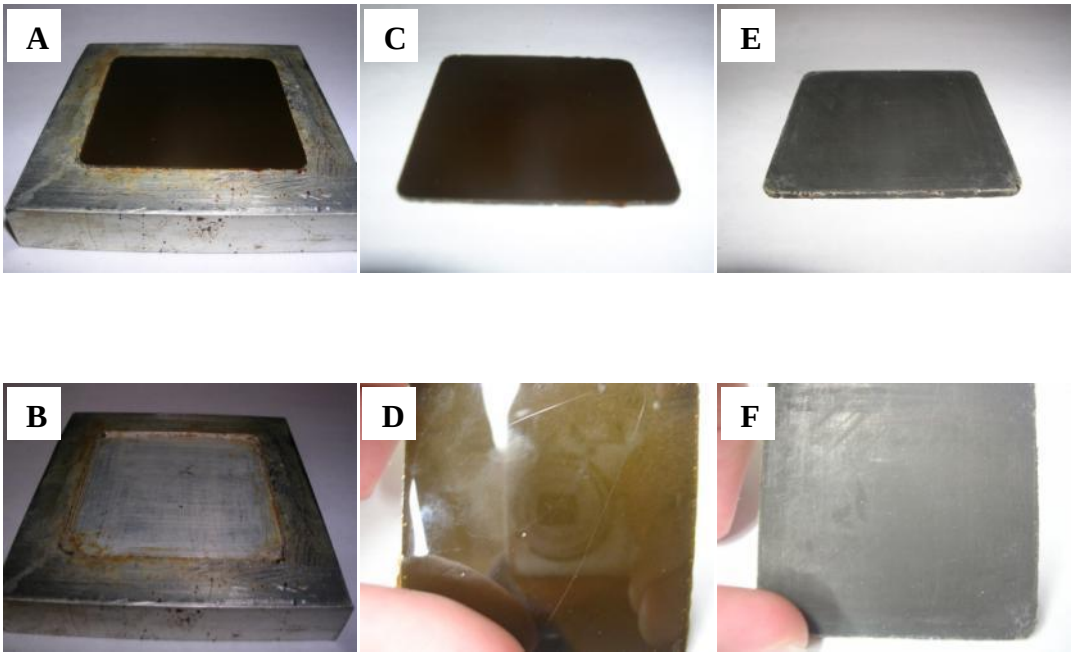

Figure 10: Pictures of Epoxy Sample (A) Epoxy in mold (B) Emptied mold (C) (D) top surface (E) (F) bottom surface.

2.3.3 Epoxy composite processing with PG solvent

As previously stated, Propylene Glycol was considered as a solvent due it's reported interaction with nickel particles [19]. Nickel Nanostrands are first probe sonicated in PG for 15 minutes to coat the nickel. The solution is then added to the epoxy resin and subjected to bath sonication and mechanical shear mixing for 1 hour. The PG is then removed by heating the solution on a hot plate while undergoing continuous stirring. The curing agent is then added and the mixture is then mechanically sheared at 69˚C for several hours. The mixture is then cast into a mold, cured at 177˚C for 2 hours and then characterized if dispersion is observed visually.

2.3.4 Epoxy composite processing with no solvent

A no solvent-based approach was also pursued when processing the NiNS-epoxy composites. To create a Nickel Nanostrand epoxy without the aid of solvent, the desired amount of NiNS were added directly to the EPON Resin 862. This mixture then underwent an hour of bath sonication while simultaneously shearing with a mechanical mixer at 300 RPMs. The curing agent was then added to obtain a 20g mixture that was mechanically sheared for an additional hour at 300 RPMs. The stirred mixture was then poured into a metal mold coated with high temperature heat release agent and subsequently cured in the oven. Figure 11 shows the processing used to create a solvent free NiNS – Epoxy composite.

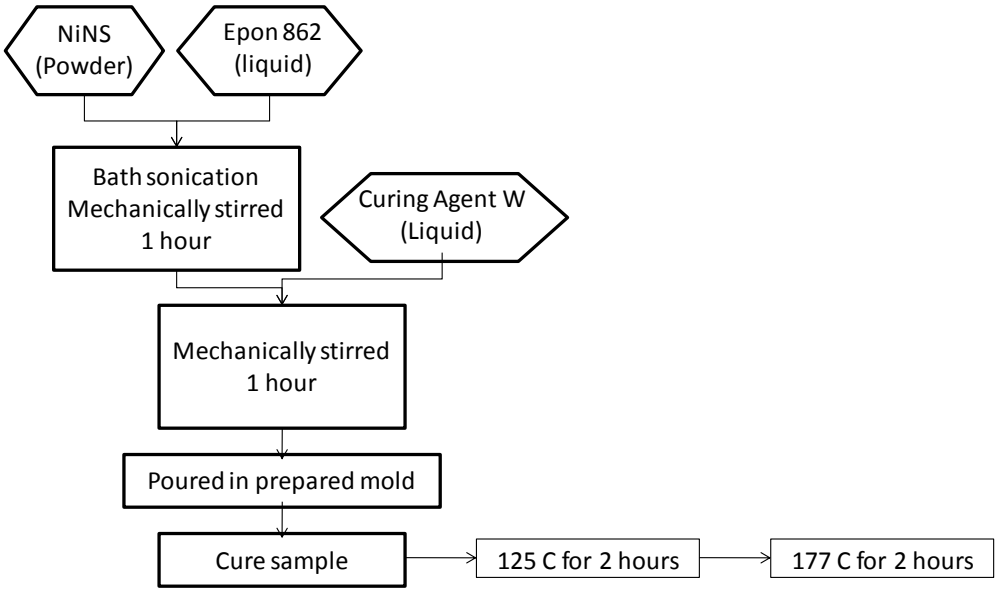

Figure 11: Solvent free NiNS – Epoxy processing chart

Using OM to examine the through-thickness dispersion, it was determined that the planar dispersion was still good but the some NiNS have settled. After varying some of the parameters, dispersion improved particularly after increasing the mechanical shearing time, the step following addition of the curing agent W, to 24 hours and heating the sonication bath to 69˚C during this time. In addition, fifteen minutes of bath sonication and mechanical shearing were added at the end of the mixing to degas the solution, and the high temperature steps were altered. For example, the two-hour cure rate at 125˚C was removed. It is noted that the increased mixing time produced a very viscous mixture that starts to harden when removed from the elevated temperature bath. Because of the high viscosity, the epoxy is spooned into the mold rather than poured. Small settling was seen near the top and bottom layers of the samples so the mechanical shearing was increased to 30 hours. This modified processing resulted in good dispersion throughout the entire thickness. Using this procedure, pristine epoxy as well as multiple NiNS nano-composite samples were made, tested and compared using DSC, DMA and DS. Processing charts for the 30 hour mixing times are shown in Figure 12.

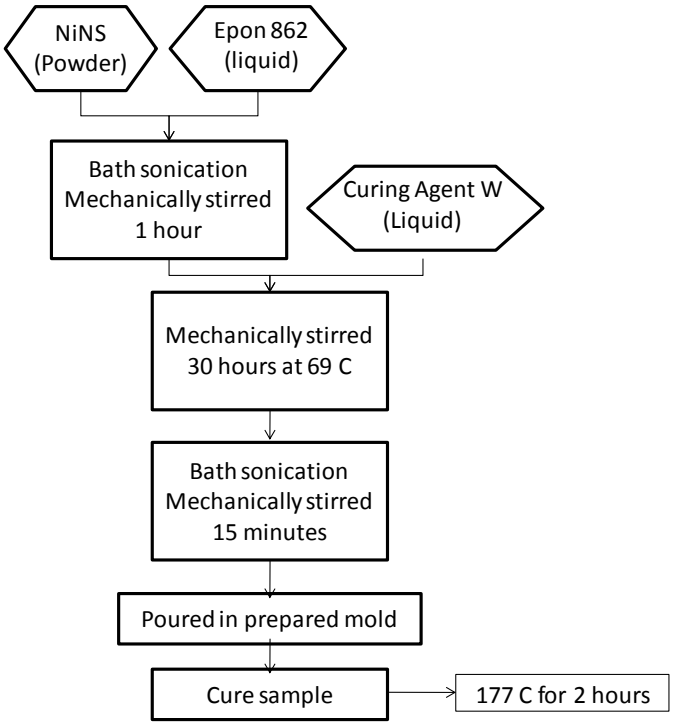

Figure 12: Solvent free NiNS – Epoxy processing chart (30 hour mixing)

2.3.5 PVDF composite processing with DMAc

To process a NiNS – PVDF nano-composite, NiNS were first probe sonicated with DMAc for 15 minutes. The solution was added to a beaker containing more DMAc and was bath sonicated and mechanically mixed for 5 minutes before adding PVDF to the mixture. After 15 minutes of shear mixing and bath sonication at 69 °C, the solution was placed on a hot plate at 200°C while continuously undergoing shear mixing. This elevated temperature causes the DMAc to rapidly evaporate while melting the PVDF and turning the mixture from a dissolved PVDF solution to a melt solution containing small amounts of DMAc. The solution is then poured into a metal mold as well as cast on a glass

plate as a film. Both mold and glass plates are then both placed in an oven preheated at 130°C to ensure complete evaporation of DMAc. PVDF begins to solidify after a few minutes in the oven, trapping the dispersed NiNS. Figure 13 shows this process.

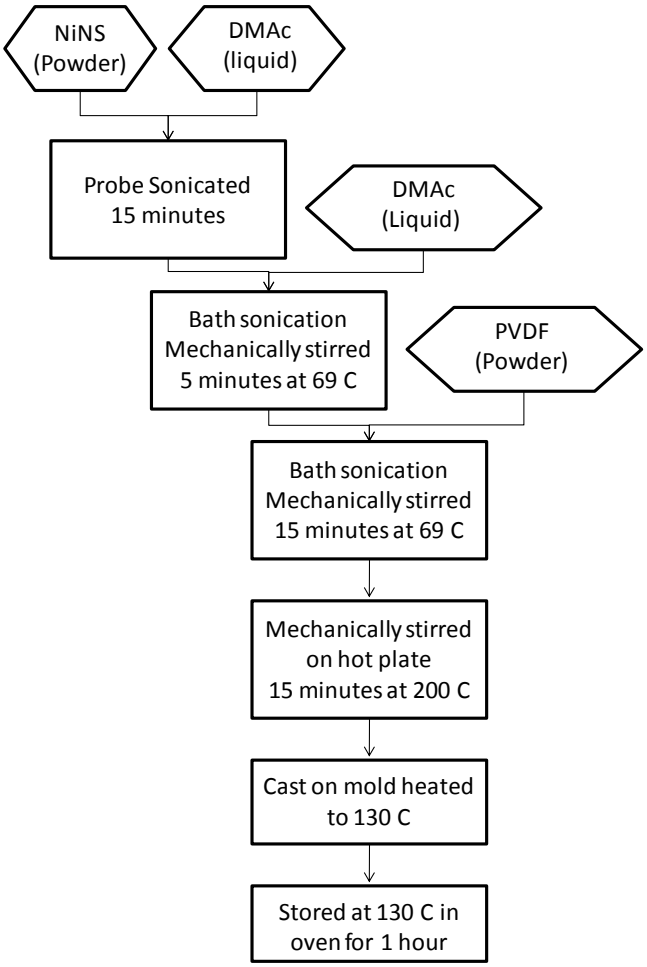

Figure 13: NiNS - PVDF with DMAc processing chart

2.3.6 PVDF composite processing with PG solvent

In an attempt to further enhance the dispersion of the NiNS in the PVDF solution melt, PG was used in place of DMAc. The NiNS and PVDF were processed in the same manner as was discussed in the previous section with the PG in place of the DMAc solvent.

2.4 Characterization of nano-composite films

To study and determine the dispersion and effects of NiNS nano-composites each sample must be characterized. This section describes the instruments used to determine mechanical, thermal, electrical and optical properties and include Optical Microscopy, Dielectric Spectroscopy, Differential Scanning Calorimetry, Dynamic Mechanical Analysis and Fourier Transform Infrared spectroscopy.

2.4.1 Optical microscopy

The Optical Microscope used was an Inverted Zeiss® transmission optical microscope. A transmission OM beams light through the sample and allows for visually determining dispersion of fillers within the matrix. By adjusting the focal point of the microscope, it is possible to view different depths within the composite. A Carl Zeiss AxioCam was used to record digital images of the magnified composite.

2.4.2 Differential scanning calorimeter

The Differential Scanning Calorimeter, or DSC, used to test composite samples was a TA Instruments Q20 DSC. These instruments use a form of thermal analysis used to detect thermal phase transitions. In DSC, a sample is heated linearly alongside a reference sample. The instruments measures the amount of heat required to keep both samples at nearly the same temperature. When a phase transition occurs over a temperature range, a difference in heat flow will be recorded and, depending on whether the process is endothermic or exothermic, will show an increase or decrease in the flow. The samples used in this research were cut down to approximately 10 mg and encased in aluminum t-zero pans and lids. Several characteristic material properties can be observed from this characterization method such as percent crystallization, melt temperature, glass transition temperature (T_g) and thermal degradation. By observing the changes in these properties, the effect of adding nano-fillers to the matrix can be better understood. To erase any effect of thermal history, a sample is heated to the desired maximum temperature and then cooled down to the original temperature. This cycle is repeated again to record the heat flow after its thermal history has been erased by the first cycle.

2.4.3 Dielectric spectroscopy

A Novocontrol® Dielectric Spectrometer was used to record the electrical properties on composite samples. The spectrometer uses a two-electrode configuration by implementing the ZGS extension shown in Figure 14. Dielectric Spectroscopy is used in this study to determine the electrical conductivity, dielectric constant and the phase angle across a frequency range from 10^{-2} Hz to 10^{7} Hz. A temperature sweep is also performed under a constant frequency. An AC electrical field applied across the two-electrode configuration interacts with the samples electric dipole moments. The dielectric constant represents the electrical charge stored by an insulating material relative to that stored in a vacuum. The electrical conductivity is a measure of a materials ability to conduct an electrical current across an area through the thickness, measured in Siemens per meter. The tan(δ) is a measurement of the dissipation of electromagnetic energy. The composites to be tested are first cut to an appropriate size and then polished down to remove any air pockets or other surface defects that may interfere with correct measurements. Typical sample sizes used were 15mm by 15mm with a thickness dependent upon the material being tested. The samples are coated with high purity SPI® Silver Paint that acts as an electrode.

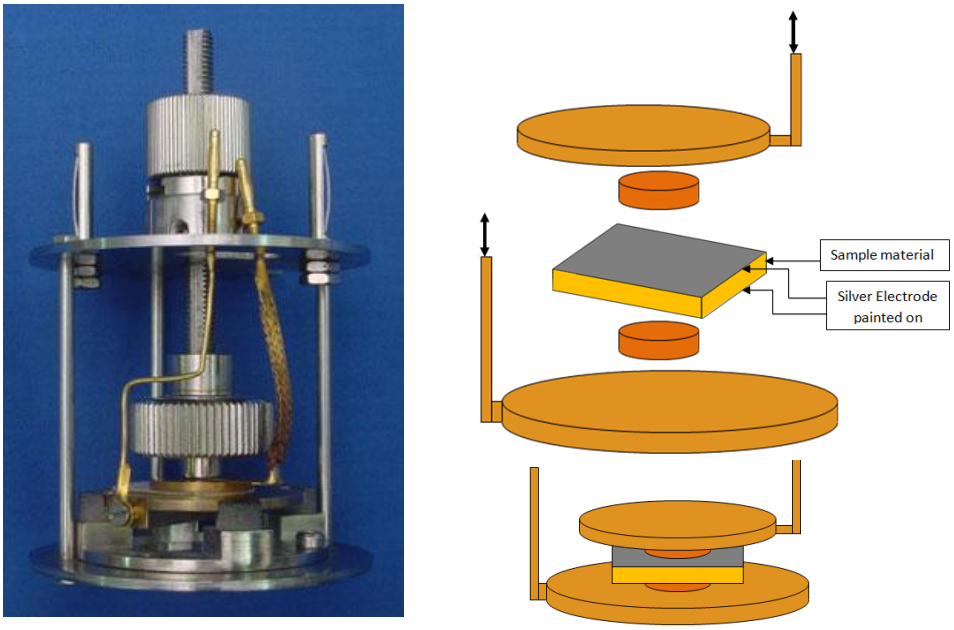

Figure 14: Dielectric Spectroscopy sample configuration

2.4.4 Dynamic mechanical analysis

The Dynamic Mechanical Analyzer, DMA, used to test composite samples was a Rheometric Series RSA (Rheometrics System Analyzer) III. The RSA III has a strain resolution of ± 0.05µm, a phase angle resolution of ± 0.1˚ and a temperature range from -150˚C to 600˚C. All samples were tested at a 1 Hz frequency. The DMA can be used to characterize the dynamic mechanical properties of a polymer by running a strain controlled dynamic temperature ramp test which applies a sinusoidal displacement and measures the resultant stress. In a perfectly elastic material, the applied stress and resultant strain will be in phase with one another whereas a viscoelastic material displays a phase angle shift up to 90 degrees. The relevant measurements obtained from the DMA are

the storage modulus, loss modulus, and the phase angle, tan(δ), where δ is the aforementioned phase angle shift. The storage modulus, E', represents the amount of elastic energy the material can store while the loss modulus, E'', represents its ability to dissipate energy. Tan (δ) measures the damping ability of the material. Equations 2.1 – 2.3 display how these properties are dependent on each other, stress (σ) and strain (ε).

$$E' = \frac{\sigma}{\varepsilon}\cos(\delta) \tag{2.1}$$

$$E'' = \frac{\sigma}{\varepsilon}\sin(\delta) \tag{2.2}$$

$$\tan(\delta) = \frac{E''}{E} \tag{2.3}$$

Using DMA, one can determine the glass transition temperature (T_g). When a polymer reaches temperatures near its T_g, the storage modulus has a dramatic drop in value whereas the loss modulus reaches a maximum. Past the T_g, both properties drop and quickly stabilize to a new value. Near the onset of T_g, tan(δ) begins to trend upward and will eventually peak, decrease and then stabilize again. By studying the results of T_g, E', E'', and tan(δ), the effects of filler on the composite behavior can be better understood. In the case of as-cast films, a thin film extension fixture was used whereas bulk samples with larger thickness (0.2 mm and higher) used a three-point bending fixture. Both fixtures are shown below in Figure 15. For a film sample, the average dimensions were 35mm long, 6 mm wide and between 0.04-0.20 mm thick. The bulk samples were 45 mm long, 6 mm wide and between 0.8 – 1.3 mm thick. Variations in thickness and width throughout the sample length have the potential to cause

large inaccuracies; therefore, care must be taken when polishing or cutting a sample to achieve minimal discrepancies in dimensions.

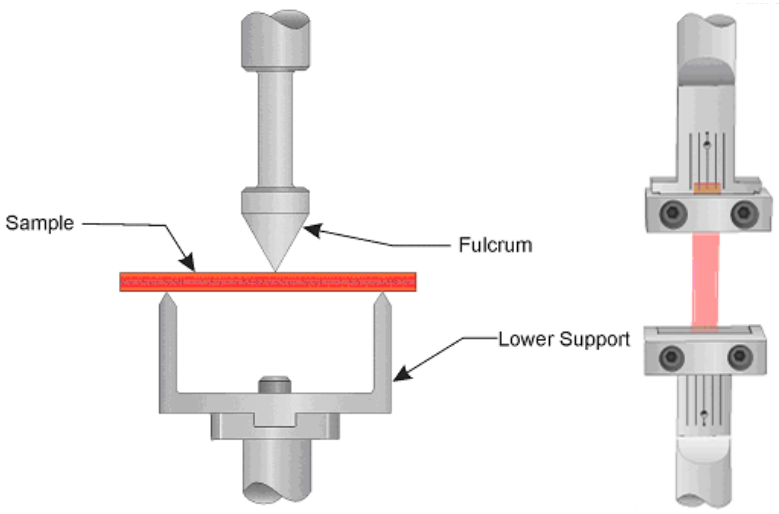

Figure 15: DMA sample configuration

2.4.5 Fourier transform infrared spectroscopy

Fourier Transform Infrared Spectroscopy, or FTIR, will be used to examine changes in the PVDF films caused by the addition of NiNS by an Attenuated Total Reflection (ATR) method. FTIR performs a chemical analysis of polymeric compounds by measuring the light absorbed by a sample at various wavelengths. This information is then used to identify the functional groups on polymers, detect the formation of covalent bonds and determine the crystalline phases of the polymer matrix [33].

CHAPTER III

RESULTS AND DISCUSSIONS

3.1 CP2 nano-composite results

Initial attempts in CP2 film fabrication led to samples that with non-uniform thicknesses and full of voids or, in other cases, the cast films separated into a two-phased film. It was determined that the viscosity of the solution made a large contribution to the outcome of the film and dispersion. To this extent, the amount of DMAc used in the solution was varied until a consistent dispersion was achieved with high viscosity. The high viscosity was desired to confirm polymerization and reduce the movement of NiNS particles farther. High viscosity also insured that the solution would maintain its casted shape once exposed to higher temperature. Once a consistent film was achievable and repeatable with a precise method, a 0.0, 0.1, 1.0 and 5.0 wt% NiNS – CP2 films were processed. During processing, the NiNS appeared to maintain dispersion visually to the naked eye. During the cure cycle, the CP2 decreases in viscosity until enough DMAc is evaporated and the polymer begins to harden. Following the cure cycle, the film and glass plate are kept in the oven and slowly cooled down to room temperature. The film and glass are then submerged in warm water and gently removed from the glass plate to be analyzed.

Using the OM, digital images were recorded and analyzed for the appearance of agglomerates and overall nano-particle dispersion. Due to the larger size of some of the NiNS present, the OM can be used to see general

dispersion and agglomerates. To confirm this, the NiNS that are seen at higher magnification appear to have branches and fit the 3D geometric profile associated with them. While most likely there are large amounts of NiNS present that are undetectable at this magnification, it is the author's belief that the visible NiNS give a good representation of the quality of dispersion and that any large agglomerates formed by smaller particles would start to become visible as well. Due to the high force asserted on the particles by sonication and shear mixing it can also be assumed that some of the branching may have broken off causing several smaller NiNS that do not appear as branched.

At first glance, Figure 16 appears to show that the NiNS are well dispersed and contain very few agglomerates. However, after several conductivity tests exhibited virtually no change in conductivity and dielectric constant it was determined that while good dispersion is observed on a planar field, the through-thickness dispersion is nearly non-existent. After reexamining the OM images, it was concluded that most of the NiNS had settled during the long cure cycle onto the bottom layer within the matrix creating a two-phase film.

After determining that the majority of NiNS had settled to the bottom, no more samples were made and farther characterization did not seem required. It was concluded that the large NiNS are not enveloped during the polymerization stage and are therefore not supporting the particles during the long cure processing. As the solution heated up to higher temperatures, the viscosity significantly decreased which also allowed the heavy NiNS particles to separate

and sink through the polyimide chains. Various levels of DMAc were used to decrease the viscosity but it was not deemed possible to overcome this decrease during cure as well as the weight of the NiNS and the lack of CP2 and NiNS interaction at a molecular level.

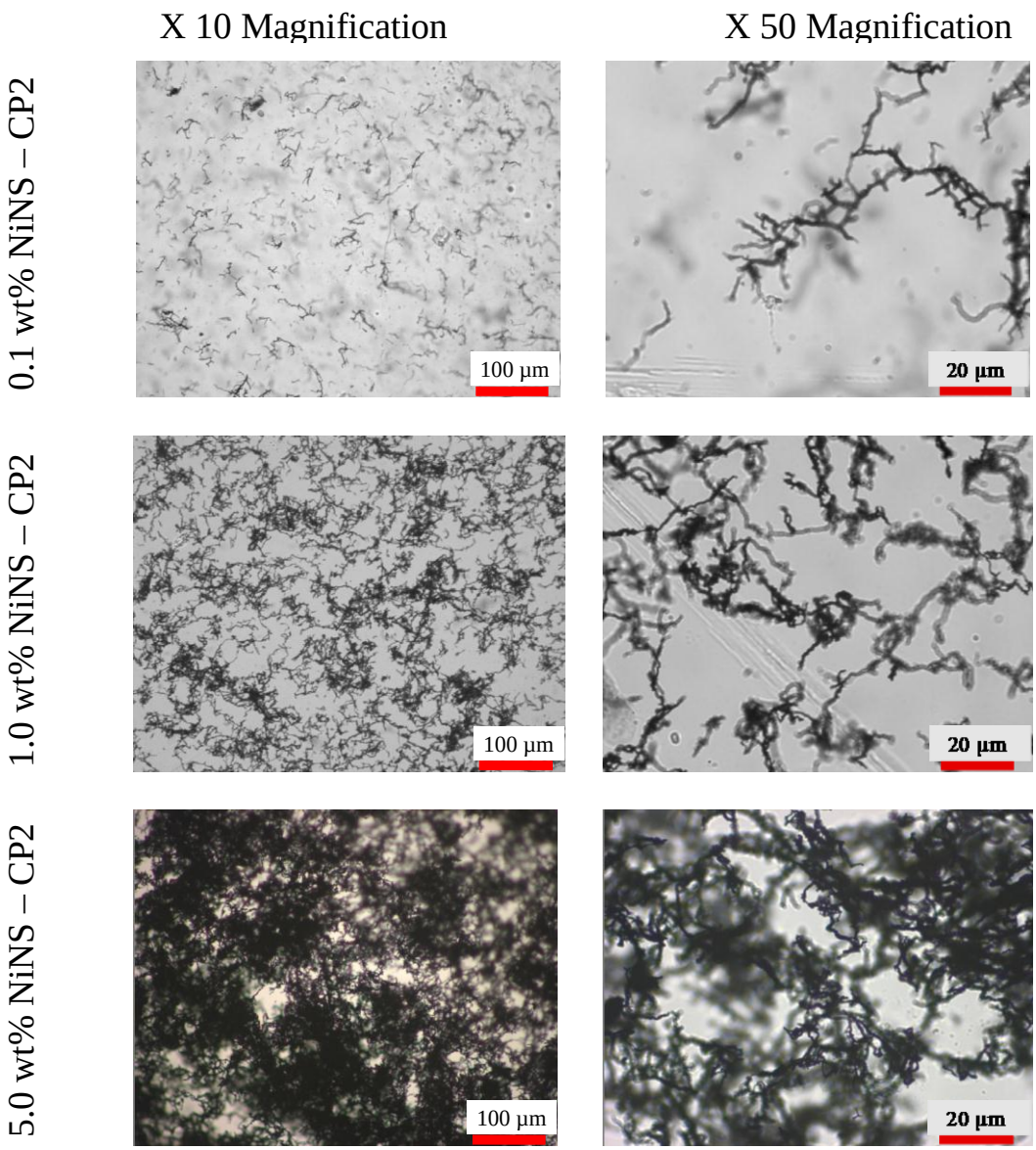

Figure 16: CP2 Optical Microscopy images

3.2 Epoxy nano-composite with DMAc solvent results

Epoxy samples were processed with DMAc using a familiar processing technique that was successful in dispersing CNFs [6]. After probe sonicating the NiNS in DMAc and shear mixing the solution with the Epon 862 resin while undergoing bath sonication, the solution appeared well disperse for a short time. The extensive amount of time required to evaporate the DMAc from the solution before adding the curing agent as well as the elevated temperature used to assist in evaporation caused the NiNS to settle on the bottom of the beaker effectively eliminating any dispersion previously enforced. Evaporation of the DMAc would often take eight or more hours to complete and the NiNS were not able to stay suspended beyond an hour. Nonetheless, in several attempts, the curing agent was introduced and the mixture was again stirred and bath sonicated for another hour. Appearing once more visually dispersed, the mixture was poured into a metal mold lined with heat release agent to aid in removing the specimen once cured. The casted mixture was then heated for four hours; two hours at 125°C followed by two hours at 177°C. Upon removal of specimen, it was observed under the optical microscope for dispersion.

The sample was viewed from the glossy top surface down to the bottom of the sample. Digital images were taken with the OM and examined as representative cross sectional dispersion in the sample. Figure 17 displays a 1.0 wt% NiNS – Epoxy composite whose images were taken from the top layer, one-third and two-third through the thickness as well as the bottom layer of the

sample. The blue squares to the left of the images represent the layer being observed and its relation to the specimen's. It is clear from these images that the majority of the NiNS have settled to the bottom of the sample during the cure cycle. Some NiNS remain on the top surface possibly due to the surface tension while smaller fragmented NiNS remained slightly dispersed throughout the rest of the sample.

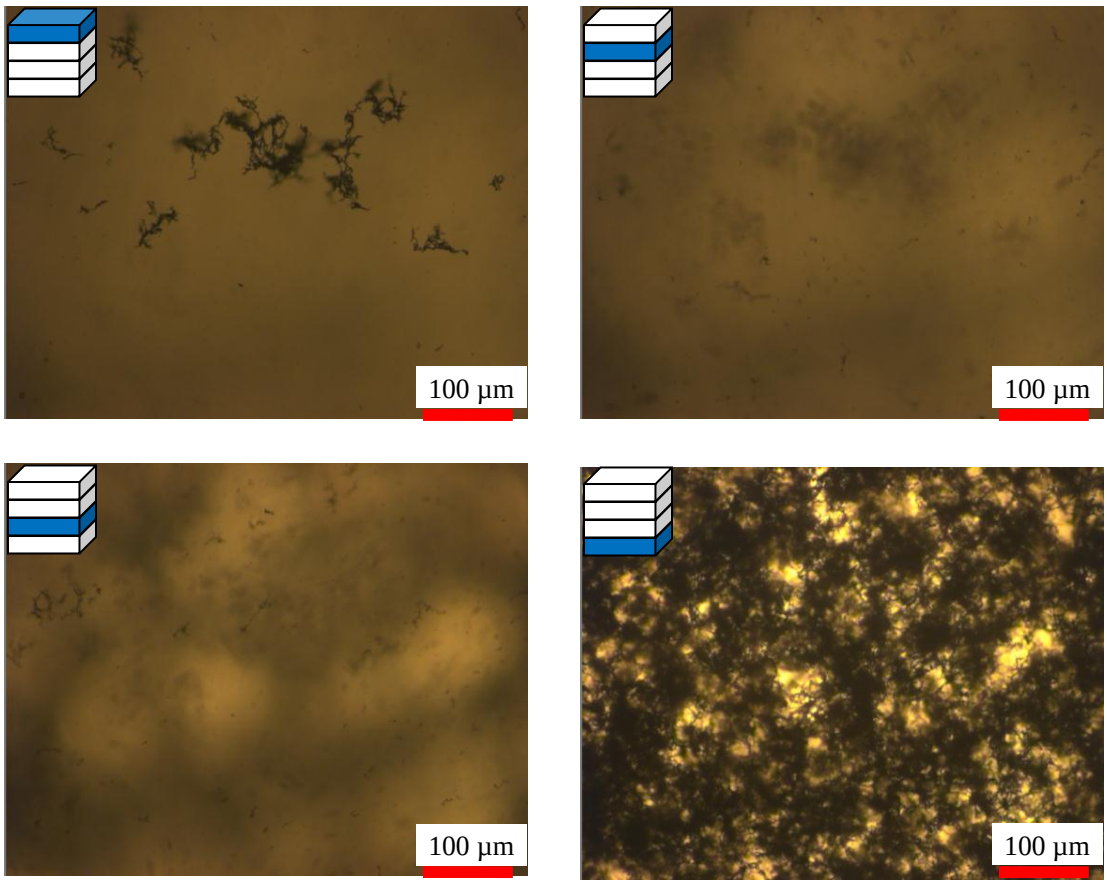

Figure 17: Optical Images of 1 wt% NiNS - CP2

It is clear from the OMs that while this processing technique worked very well for CNFs it does not work nearly as well for NiNS based nano-composites. Several impedances were observed during this process including the extended amount of time required to evaporate the solvent as well as the apparent settling during the cure cycle before the epoxy hardened. These two factors show that the NiNS do not interact in an ideal way with the epoxy molecules as the CNFs had. It became evident that this processing had to be dramatically altered beyond its initial process in order to create a well-dispersed NiNS – Epoxy nano-composite including changing the degassing method as well as the cure cycle. It was decided that the DMAc, whose sole purpose was to aid in the dispersion and break down agglomerations was causing more challenges than it had solved. Due to this drastic change in processing required, it was concluded that this technique did not deliver a dispersed film as well as desired.

3.3 Epoxy nano-composites with PG solvent results

Propylene Glycol was used in place of the DMAc solvent due to its improved interaction with the NiNS particles. When probe sonicated in PG the NiNS stayed suspended for nearly an hour before a noticeable amount began to settle as opposed to the 5-15 minutes of suspension in DMAc. After dispersing the NiNS in the PG, the solution was added to a beaker containing the Epon 862 resin and was then shear mixed and bath sonicated for an hour. Deviating from the aforementioned DMAc technique, this solution was heated on a hot plate

while undergoing continuous mixing to keep the NiNS dispersed. This was done in part due to that PG is not toxic unlike the DMAc and was easily and more rapidly evaporated. For these reasons, the PG could be evaporated under a fume hood while the DMAc had to be evaporated in a concealed vacuum oven with an attached solvent trap that did not provide a way to continuously mix the solution.

Once the PG was evaporated, the NiNS would ideally be coated with the PG increasing the suspension of the NiNS in the epoxy mixture. The curing agent is then added and the mixture is once again stirred. However, to overcome the lack of viscosity that caused the NiNS to settle in the DMAc samples, it was determined to allow the curing agent to act on the resin for an extended amount of time. Epoxy resin and the curing agent without any solvent or NiNS were mixed to determine the length of time required to notice a significant increase in viscosity that would quickly harden once exposed to the high temperature of 177 Celsius for cure. It was determined that approximately 24 hours of contact with the curing agent caused the mixture to become significantly tacky yet still liquid enough to pour and cast. When this new mixture based on the PG surfactant was used, it took less than 10 hours to harden the same resin – curing agent. This quickly hardened epoxy behaved very weak and brittle displaying a significant change in basic properties that suggested that the presence of this PG had somehow chemically altered the epoxy. After several attempts altering small parameters it was determined that while the PG showed

good behavior in suspending the NiNS, it would not allow for an epoxy sample that could be rightfully compared to pristine and tested epoxy not exposed to the PG. It is the author's belief that one better suited in chemistry could find a surfactant that shows good dispersion with the NiNS as well favorably agreeing to the polymer matrix. If a good surfactant can be found it should reasonably stand that this method used has the potential to successfully disperse NiNS in epoxy. OM images and other characterization techniques were not used in this process due to the highly brittle state of the epoxy.

3.4 Epoxy nano-composites without solvent results

Without a clear surfactant or solvent to use in the processing of a NiNS – epoxy composite an attempt was made to create a sample without the use of these aids. After shear mixing and bath sonication of NiNS directly added to the Epon 862 resin, the curing agent was added and mixing continued for 24 hours to achieve the tacky mixture that could still be poured and cast. As shown in the next section there was a small degree of NiNS settling that occurred yet it was vastly improved compared to the previous epoxy results that had incorporated DMAc. Another mixture was tested but with 30 hours of mixing time rather than the previous 24 hours. This mixture no longer had the ability to be poured into the sample mold as its viscosity increased dramatically when cooled down to room temperature.

To overcome this obstacle, a simple spatula was used to scoop up the mixture at elevated temperature and then spread onto the mold. While this method seems rather unorthodox it is the author's belief that this process could be better implemented in industry where the equipment to heat a mixture and cast it would be one in the same not requiring the mixture to be exposed to room temperature for prolonged times such as is the case with the method used here.

Once placed in the mold, the mixture is then heated in an oven at 177 Celsius for two hours. Due to the prolonged exposure to the curing agent, it was deemed no longer necessary to allow for increased interaction between the resin and curing agent during the previously mentioned two-hour cure cycle at 125 Celsius. Once the epoxy is heated, the viscosity lowers which allows the epoxy to flow into the shape of the mold. With a sample appearing well dispersed more samples were processed and characterized containing 0.0, 0.1, 1.0, 2.5, 5.0 and 10 wt% NiNS. For comparison purposes, Table 1 displays the respective volume concentration of the NiNS. The density of Nickel is 8.91 g/cm^3 whereas epoxy has a density of 1.14 g/cm^3.

Table 1: Sample concentrations of NiNS in Epoxy

wt% of NiNS	0.0%	0.1%	1.0%	2.5%	5.0%	10.0%
vol% of NiNS	0.00%	0.01%	0.13%	0.33%	0.67%	1.40%

Polished samples from 0.0 wt% to 5.0 wt% are shown below in Figure 18 laying on a piece of white paper to show the change of opacity from light yellow to dark black as the wt% of NiNS increased.

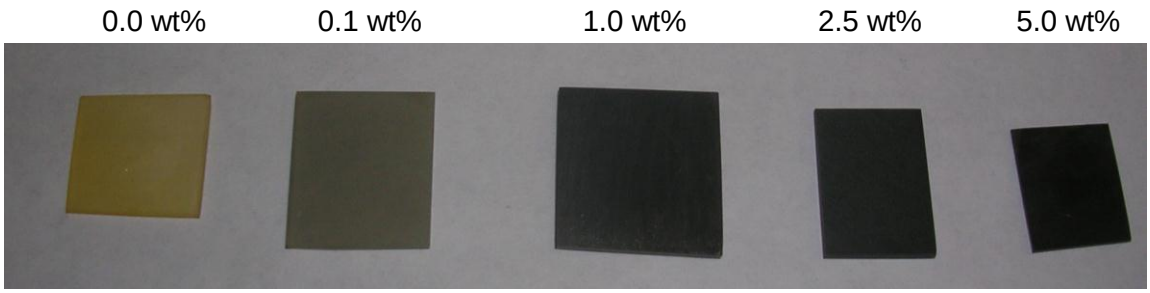

Figure 18: Digital images of polished NiNS - Epoxy nano-composites

OM images were again taken from the top surface down to the bottom. Composites consisting of 2.5 wt% or higher NiNS in epoxy contained too many NiNS for meaningful images due to the limited light allowed through the thick samples. The 1.0 wt% composites can be observed with bright light but many shadows are also seen. These shadows that are visible are NiNS in different layers of the composite that are currently not in focus. By ignoring the shadows and looking only at the NiNS that are in focus it is possible to determine the distribution of NiNS throughout the thickness by comparing multiple still images.

Figure 19 displays six images of a 1.0 wt% sample that was mixed with the curing agent for 24 hours. Figure 20 displays a 1.0 wt% sample after being for 30 hours while Figure 21 displays the through thickness images a 0.1 wt% sample after the same 30-hour procedure.

The 1.0 wt% that had underwent 24 hours of mixing with the curing agent, shows a seemingly good dispersion. Upon closer examination, the top layers are slightly sparser while the lower samples appear more clustered and make it difficult to see through the shadows of other NiNS. The 1.0 wt% composite that underwent 30 hours of mixing is slightly more transparent due to a lack of clustered NiNS on the bottom layer. There appear to be less NiNS on the top layer of the composite but it quickly begins to even out. The 0.1 wt% NiNS – epoxy sample best exemplifies the through thickness dispersion of the NiNS. It appears that the NiNS are evenly dispersed in each plane as well as through the thickness while also showing very little agglomerations from the NiNS.

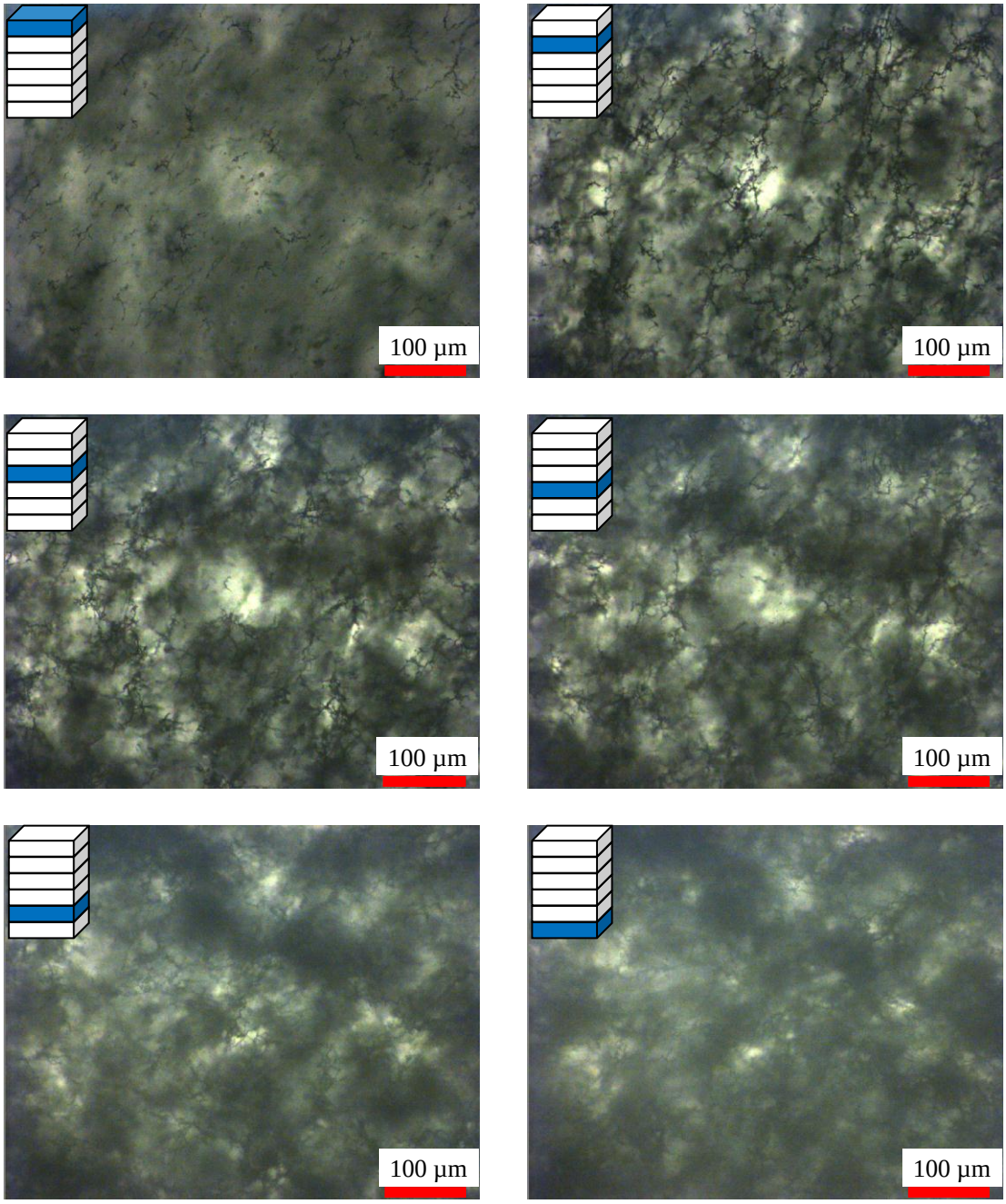

Figure 19: OMs of 1 wt% NiNS - Epoxy with 24 hours of mixing

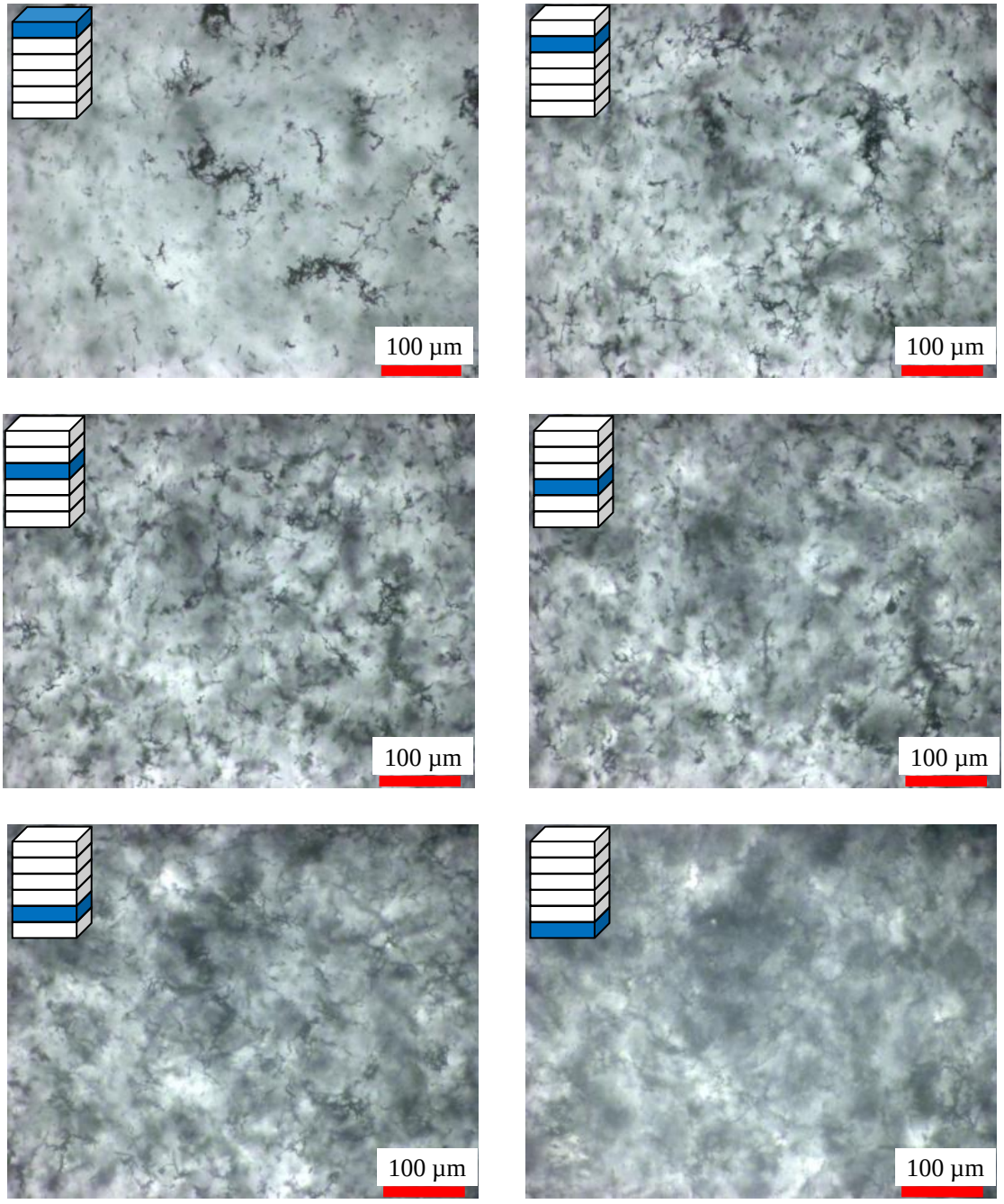

Figure 20: OMs of 1 wt% NiNS - Epoxy with 30 hours of mixing

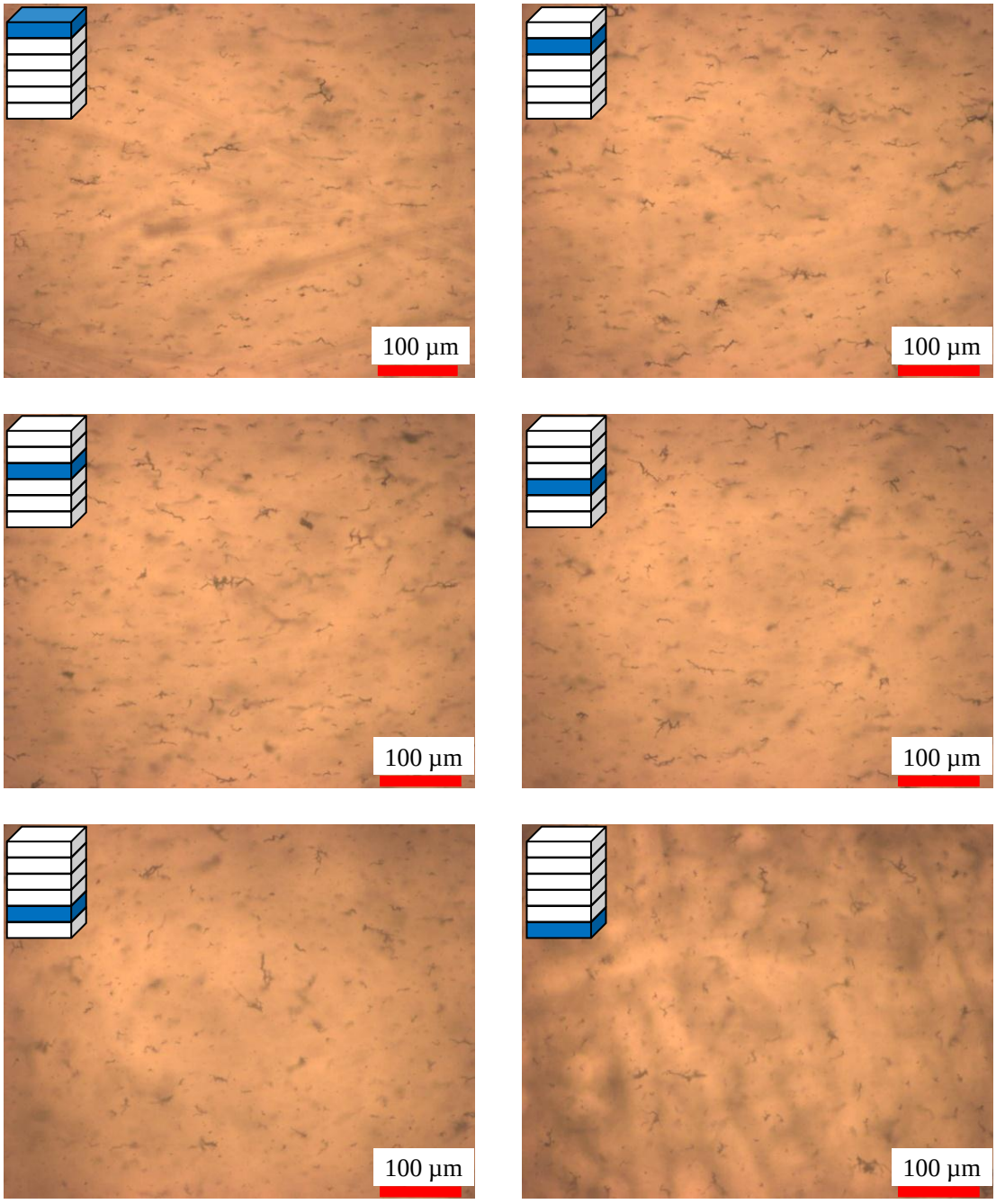

Figure 21: OMs of 0.1 wt% NiNS - Epoxy with 30 hours of mixing

DMA measurements were performed on three samples for each specimen. To determine the characteristics over a range of temperature, a temperature ramp, which measures the samples in specified time intervals while maintaining a steady increase in temperature, was used. Due to this method, which causes measurements to be taken at non-specific temperature intervals, the results displaying the best representative samples were used for comparison in all following figures. Comparing the storage modulus between all samples, as displayed in Figure 22, reveals that the moduli are relatively close to one another at temperatures below T_g. Transitioning through the T_g, a drop in the storage modulus is experienced as is expected. By observing the relative location of the decrease near T_g, it can be seen that the 0.1 wt% and 2.5 wt% sample begin to decrease significantly before any other samples. The reason for this is not known since all the samples were processed identically. After this transition and above 1 wt%, the storage modulus increases with an increase in the NiNS wt%.

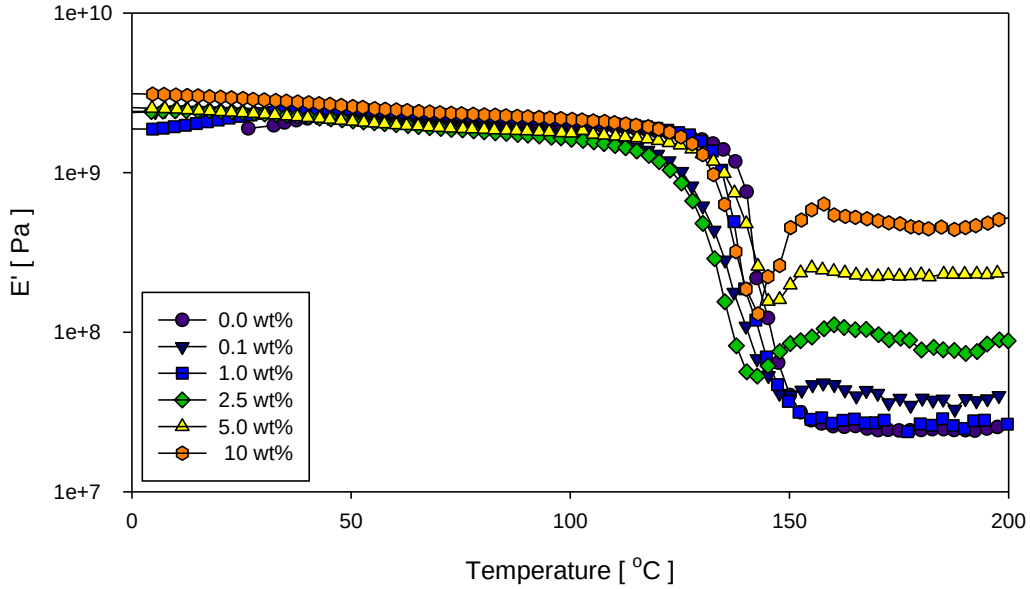

Figure 22: Storage Modulus at Room Temperature

A comparison between the different samples is more easily observed by comparing the properties near two temperatures, one below and one above T_g. Figure 23 displays the representative storage modulus near 40°C, which is well below the glass transition temperature. All values are between 2 and 2.75 GPa with a small increase in the storage modulus with increasing weight percentage. Due to such a small change in the modulus, it is difficult to definitively state any significant trend below T_g. Above T_g at a temperature of 175°C, it is observed in Figure 24 that a steady increase occurs beyond 1 wt%. A significant increase is seen from approximately 25 MPa at 0 wt% to near 475 MPa at 10 wt%.

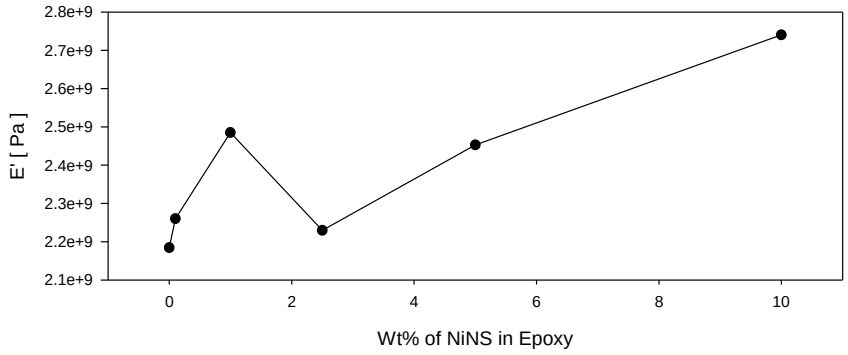

Figure 23: Storage Modulus at 40°C

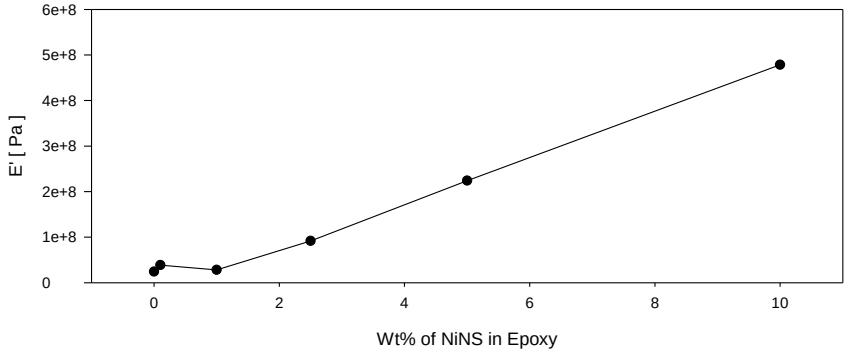

Figure 24: Storage Modulus at 175°C

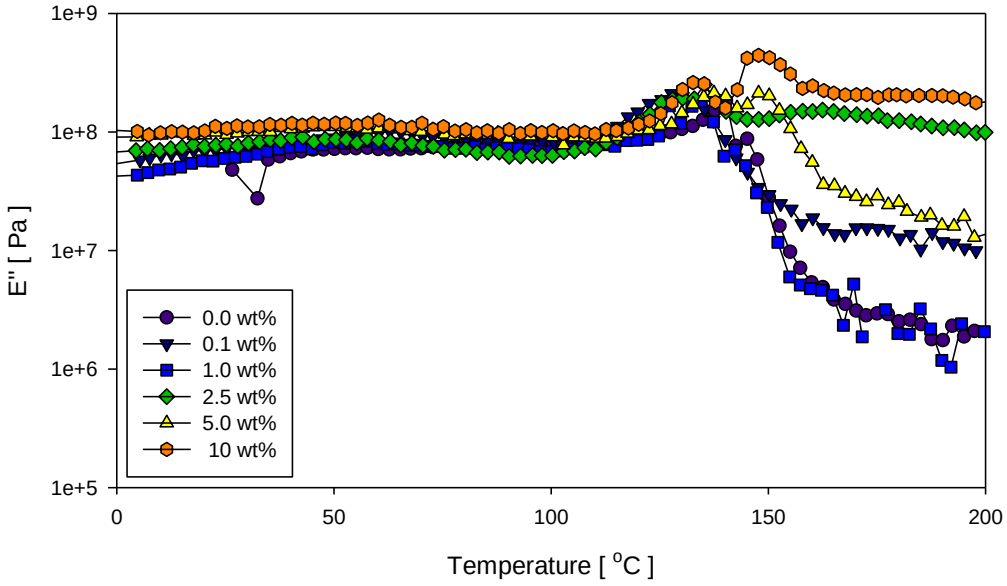

Figure 25: Loss Modulus at Room Temperature

Sample representative values for the loss modulus are displayed in Figure 25 while Figure 26 and Figure 27 focus on temperature values below and above T_g. Before T_g is reached, a small but noticeable increase in the loss modulus is seen with increasing NiNS concentration. Above T_g, a significant increase near 2 magnitudes can be seen between 0 and 10 wt%.

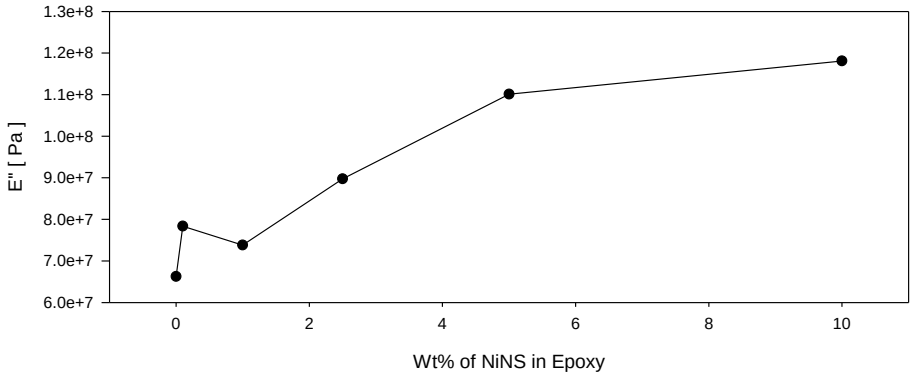

Figure 26: Loss Modulus at 40°C

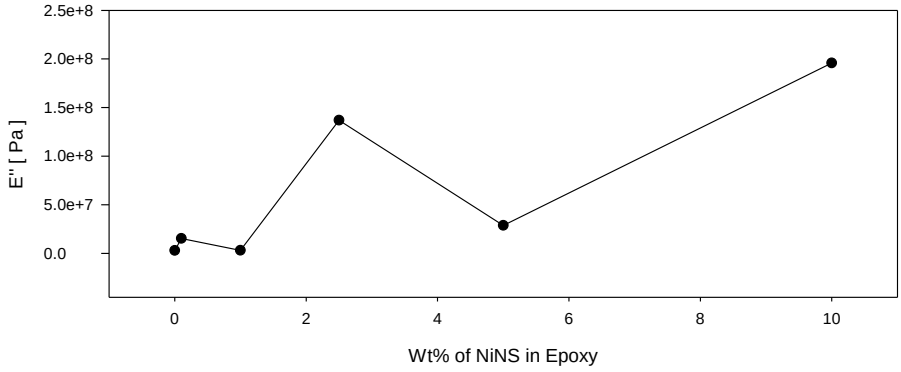

Figure 27: Loss Modulus at 175°C

Figure 28 display a representative tan(δ) value for all tested composites. Upon reaching T_g, a large increase is seen. Once the test samples are done

transitioning through the T_g, the tan(δ) values level out, in some cases at an increased value. No direct pattern is observed between the various samples after T_g other than the 2.5 wt% being much larger than the other concentrations perhaps indicating error in the test sample.

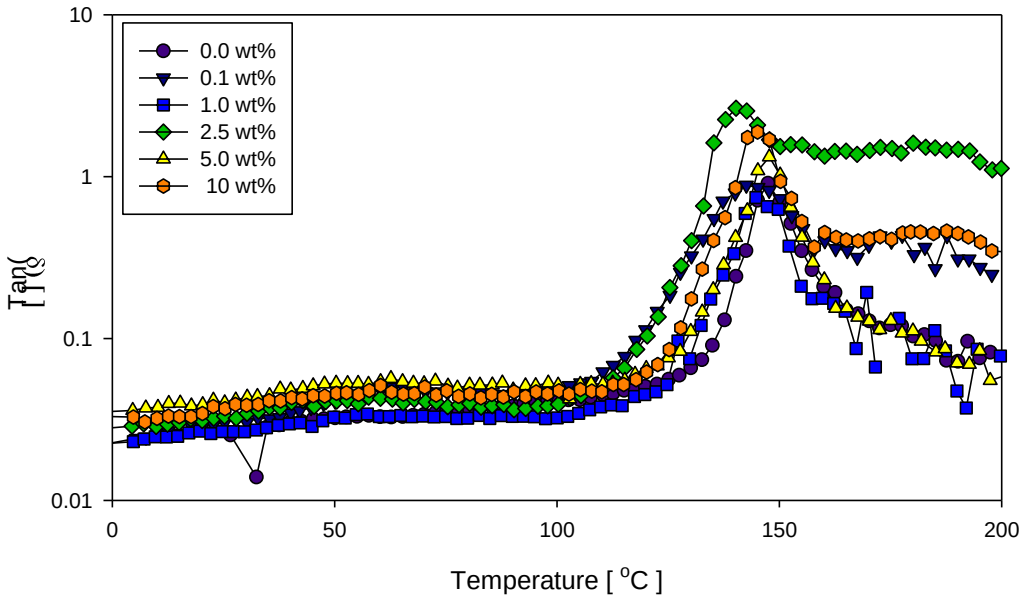

Figure 28: Tan(δ) at Room Temperature

DSC testing on the NiNS – epoxy nano-composites was performed using a heating ramp of 10°C/min and cycled from 40°C to 200°C twice. The second heating and cooling cycle is then used to determine the T_g of the composite using the given software. Use of the second cycle allows for a measurement that is independent of the samples previous heat profiles. Figure 29 displays the second heat cycle of a 0.1 wt% NiNS – epoxy sample for reference. Near the T_g,

a drastic decrease in the heat flow is observed which begins to stabilize shortly thereafter. The inset shown below for the 0.1 wt% nano-composite shows an inflection point at 141.40°C indicating the glass transition temperature.

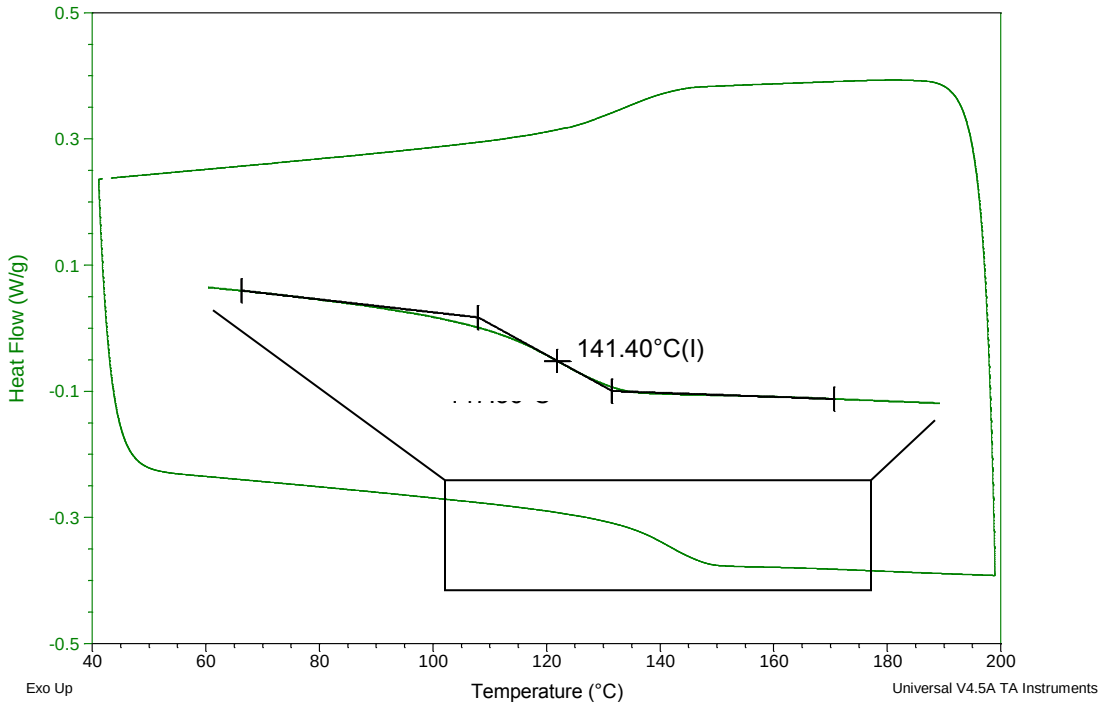

Figure 29: DSC of 0.1 wt% NiNS - Epoxy nano-composites

All wt% samples for the NiNS – epoxy were tested using the DSC with the same heat profile. Table 2 displays the measured T_g from the second cycle as well as the deviation in T_g from the pristine epoxy sample. Not all samples show a large enough deviation from the pristine sample to indicate a relevant change nor is there an appreciable pattern that can be deduced. It should be noted that once again, the 2.5 wt% sample deviates from the rest; it is the only sample

displaying an increase in the T_g. Disregarding this sample, the trend would support a general decrease with a NiNS additive.

Table 2: DSC results NiNS - Epoxy nano-composites

NiNS in Epoxy	Tg	ΔTg from 0.0 wt%
0.0 wt%	145.12	0.00
0.1 wt%	141.40	-3.72
1.0 wt%	143.69	-1.43
2.5 wt%	146.96	1.84
5.0 wt%	142.97	-2.15
10 wt%	139.03	-6.09

Each composite had three samples that were tested via dielectric spectroscopy. Each sample had the top and bottom layers polished away to remove any defects before adding a thin conductive silver layer on each side. The average values obtained for each composite is compared in this section. The dielectric constants for all samples are shown in Figure 30 while Figure 31 omits the 10 wt% sample to better compare the other samples. It can easily be seen that as the NiNS wt% increases, the dielectric constant also increases. There is a large increase from 5 wt% to 10 wt%, which would indicate the presence of the percolation threshold within that region.

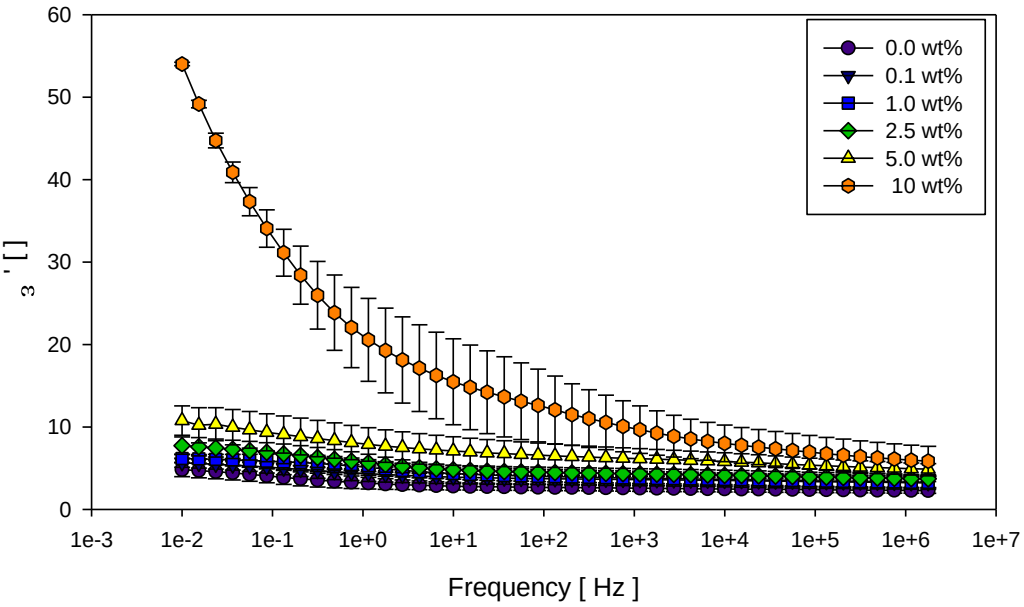

Figure 30: Dielectric Constant at Room Temperature

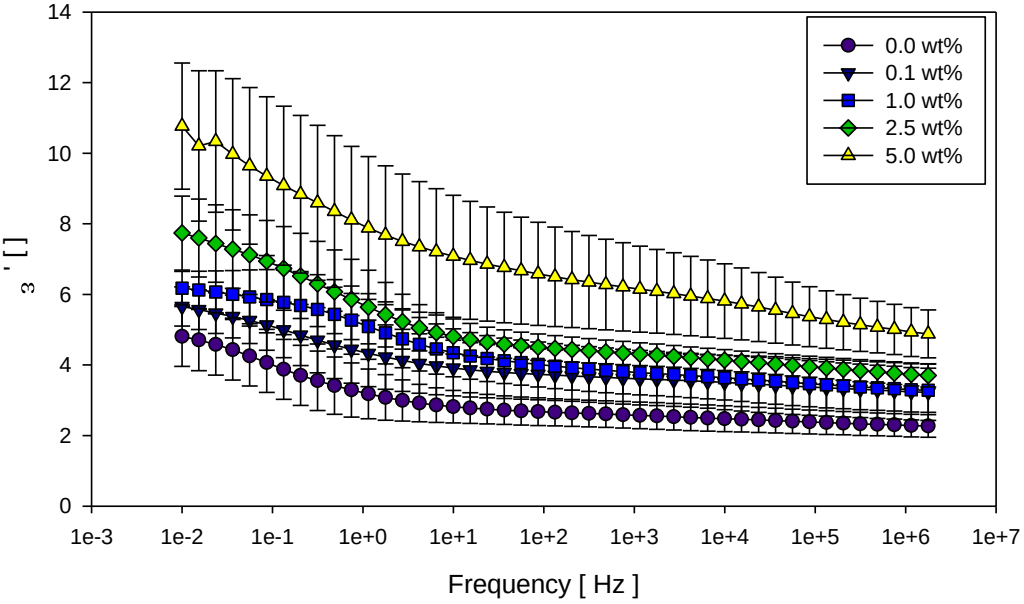

Figure 31: Dielectric Constant omitting 10 wt%

Figure 32 compares the dielectric constant measured at 1.15 kHz between all the samples. A steady increase is observed that indicates a clear increase in the dielectric constant with increasing NiNS presence. The steady progression observed along with the small error bars suggest that the NiNS are being evenly distributed throughout the sample. Alternatively, large error bars would indicate the possibility of a multiple phase solution.

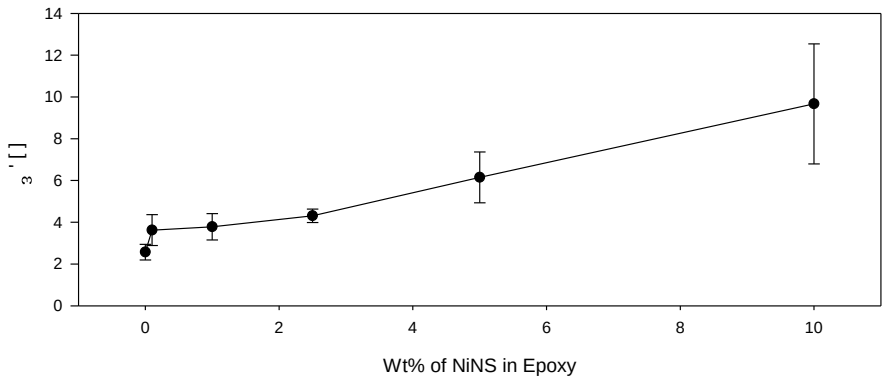

Figure 32: Dielectric Constant at 1.15 kHz

Thermal sweeps on the epoxy nano-composites using a frequency of 1 kHz from 20°C to 200°C were performed to determine the effects that may result when used in higher operating temperatures. Any changes to the dielectric constant due to the onset of T_g are also easily observed. Figure 33 displays the average dielectric constant for 3 samples of each nano-composite. Comparing the values below T_g, the composites with a concentration up to 2.5 wt% are relatively the same with only a small increase observed from the 2.5 wt%. These

lower concentrations also do not change behavior until 120°C where a sudden increase in value is consistently observed. Although an increase is observed by all these samples, they remain close enough to each other to remain within the experimental error therefore suggesting that a real consistent and observable difference is not present.

Observing the 5 and 10 wt% samples the dielectric constant decreases slowly until its T_g is approached at which point an increase is seen once again. It is of note that the 10 wt% samples gave a large degree of error when compared to the other samples. This could indicate that the 10 wt% samples are not ideally dispersed. For the higher concentrations, it is seen that the lower temperatures give rise to higher dielectric constants that steadily decrease until T_g is reached. Near T_g, the values rise until 170°C and begin to decrease once more.

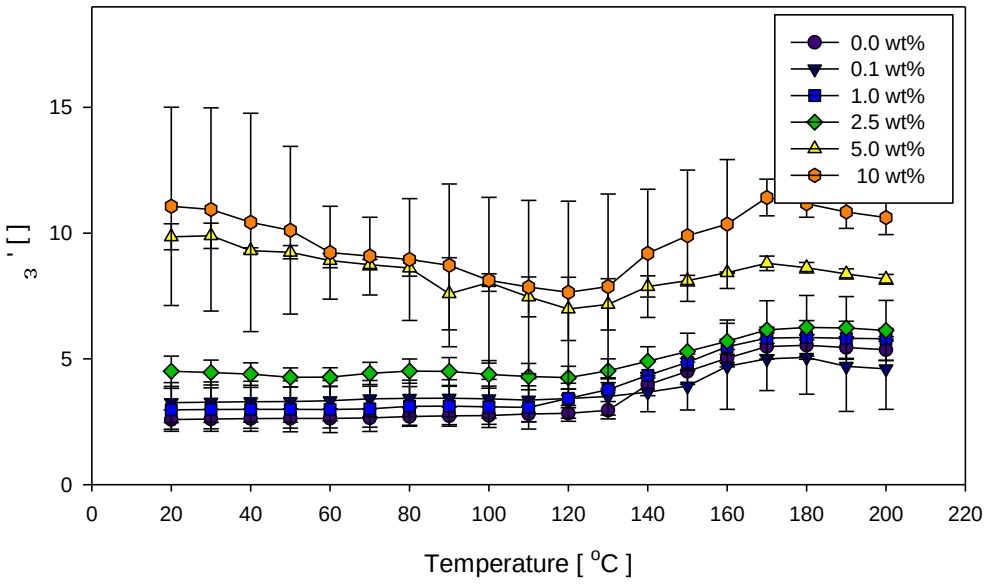

Figure 33: Dielectric Constant Thermal Sweep at 1 kHz

The conductivity shows an increasing value with an increase in concentration as seen in Figure 34. Pristine to 5.0 wt% samples show no substantial separation and all display insulating properties rather than conductive. At 10 wt%, a large increase is seen indicating an increase in the conductive properties. However, the 10 wt% sample still displays insulating properties indicating that the percolation threshold for this composite is above 10 wt%. Unfortunately, due to the non-solvent processing technique used to create these samples it became difficult to fabricate well-dispersed composites at concentrations higher than 10wt%.

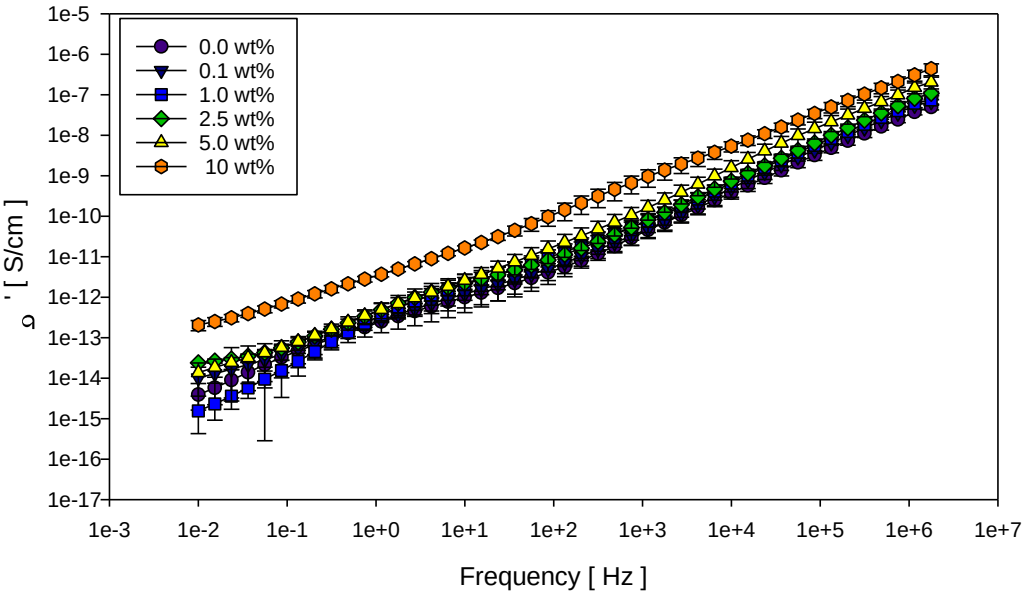

Figure 34: Conductivity at Room Temperature

Figure 35 displays the conductivity measured at 1.15 kHz versus the concentration level of NiNS in the composite. A clear increase can be seen at first, however it should be noted that the error bars observed up to 5 wt% are all within range of each other making it difficult to clearly state that an increase is observed at these low concentration levels.

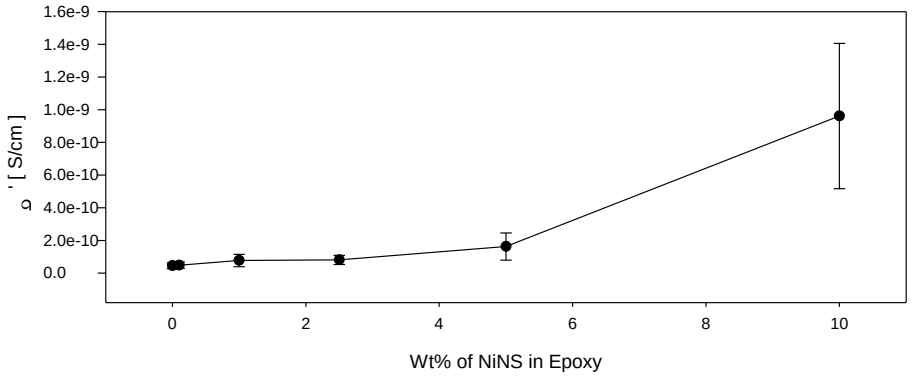

Figure 35: Conductivity at 1.15 kHz

By observing the changes to conductivity when a thermal sweep is applied, as shown in Figure 36, it can be noted that the values do not change dramatically before T_g. Near T_g, all samples appear to show an increase, most notably the low wt% samples. Past T_g, all samples appear to have a much more similar conductivity value indicating that the epoxy itself becomes slightly more conductive beyond its T_g and an addition of NiNS at this small wt% does not make a significant difference beyond this temperature.

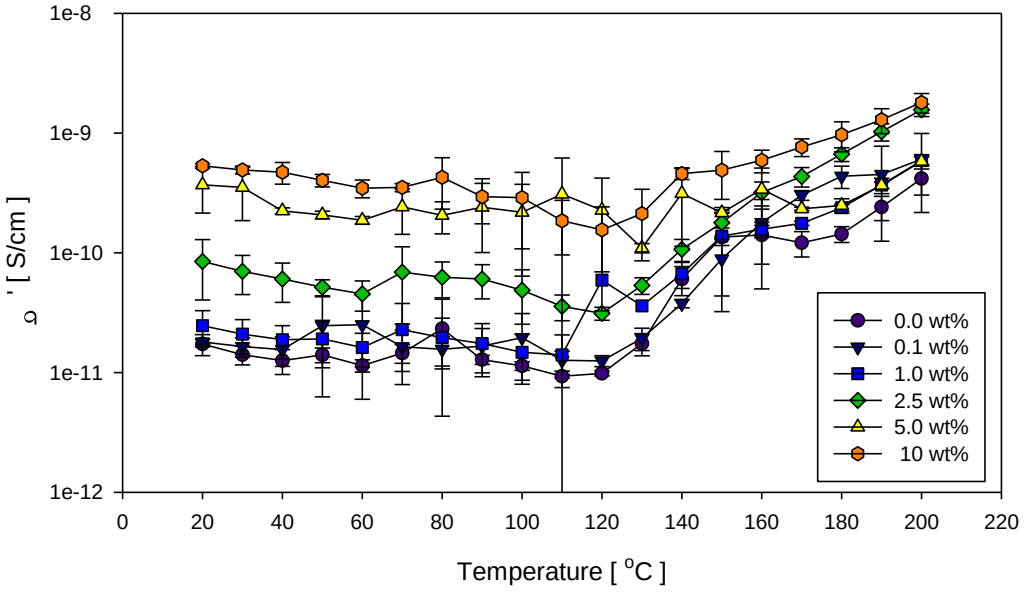

Figure 36: Conductivity Thermal Sweep at 1 kHz

Figure 37 shows the tan(δ) values for the frequency sweep of the epoxy nano-composites. show an increase in value as the concentration of NiNS increases. At lower frequencies, and for the low concentration samples, there appears to be no discernible trend and all samples appear to be similar within the standard deviation. Near 100 Hz all but the 10 wt% sample stay below a tan(δ) value of 0.1 with the 5 wt% sample slightly higher. The 10 wt% sample stays at a significantly higher value for all frequencies.

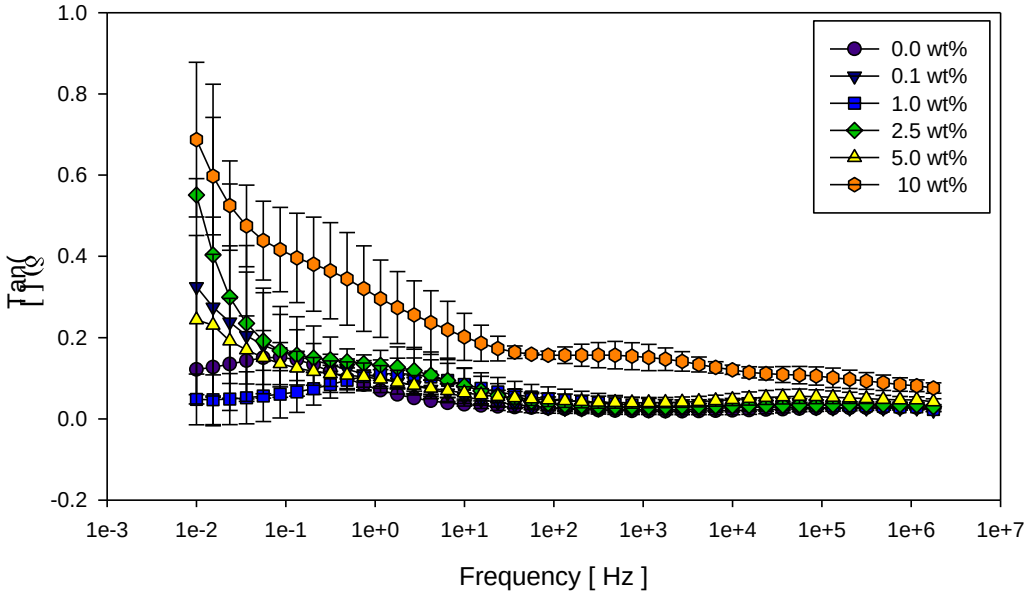

Figure 37: Tan(δ) at Room Temperature

Figure 38 examines more closely the tan(δ) values at 1.15 kHz. This figure only further shows that a large difference is not apparent until the 10 wt% sample is taken into consideration at higher frequencies.

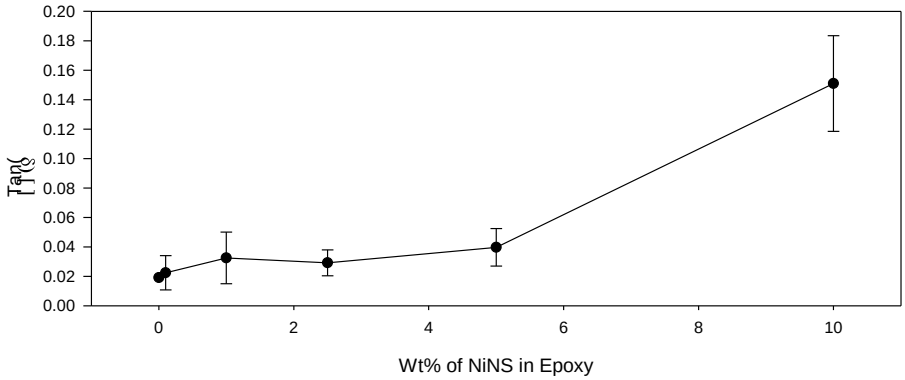

Figure 38: Tan(δ) at 1.15 kHz

Figure 39 displays the results of a thermal sweep over the samples held at 1 kHz. Below T_g, the results remain for the most part linearly and in ascending order based on NiNS concentration. Upon reaching and surpassing T_g, all tan(δ) values rise continuously but at different rates, with no appreciable pattern.

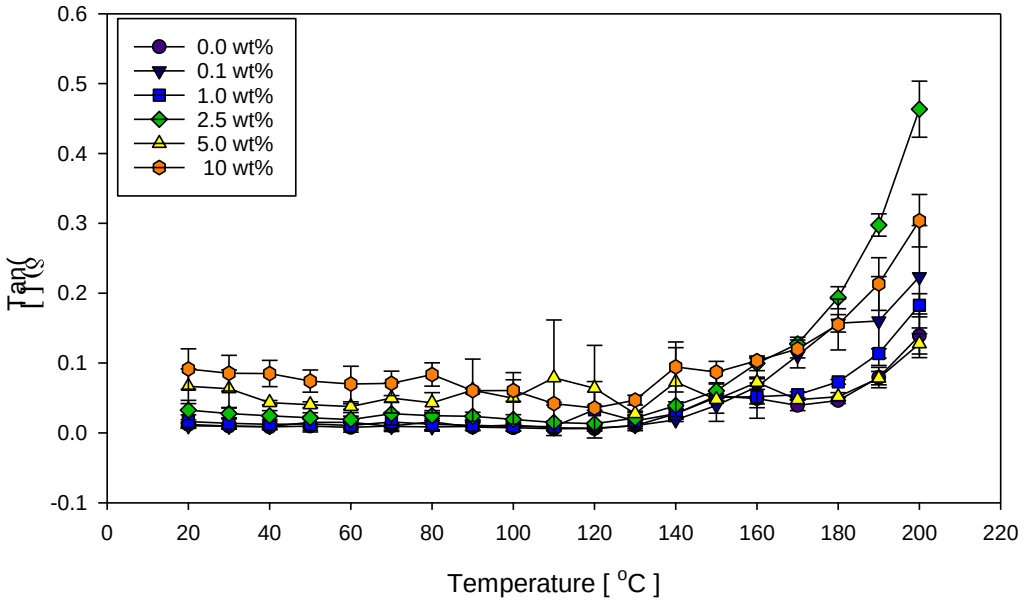

Figure 39: Tan(delta) Thermal Sweeps at 1 kHz

3.5 PVDF nano-composites with DMAc solvent results

PVDF was chosen as another thermoplastic polymer to study the dispersion of NiNS. Unlike the CP2 that was synthesized in the presence of the NiNS, the PVDF used in this experiment comes in a pre-polymerized powder. These differences between the two thermoplastics give rise to two separate processing techniques. Whereas the NiNS were introduced to the CP2 via in-situ

processing, where it was hoped that the polymer strands would grow around them, the NiNS in this case can be introduced to fully formed polymer chains in a solution or melt. When comparing the processes for both thermoplastics post casting, differences reveal a possible advantage for the PVDF-based composites. While the CP2 underwent a long cure cycle allowing the NiNS to move more freely and eventually settle, the PVDF melt solution was cooled below its melt temperature and quickly began to harden and encase the NiNS in a dispersed state. To better observe the through thickness dispersions the PVDF was cast as a thin film and in a thicker mold. Conversion of wt% concentrations to volume % based on densities are shown in Table 3. The density of the NiNS are 8.91 g/cm^3 while the density of the PVDF is 1.77 g/cm^3.

Table 3: Sample concentrations of NiNS in PVDF

wt% of NiNS	0.0%	0.1%	1.0%	2.5%	5.0%	10.0%	20.0%
vol% of NiNS	0.00%	0.02%	0.20%	0.51%	1.03%	2.16%	4.73%

Optical images were taken of the PVDF thin film to observe planar dispersion. The low thickness of the films allowed for images to be taken of all samples regardless of concentration. Figure 40 displays pristine PVDF in which the crystalline regions created during cooling can clearly be seen for comparison purposes. Films containing NiNS are displayed below in Figure 41 and Figure 42 with 10 times and 50 times magnification respectively. The crystalline regions can be observed as well as large NiNS. It can be seen that at lower

concentrations the NiNS particles appear to be more fractured but evenly dispersed. When larger concentrations are achieved, it becomes difficult to determine one NiNS from another and appear to form a coherent network. All films appear to have good dispersions and lack large agglomerates as were desired.

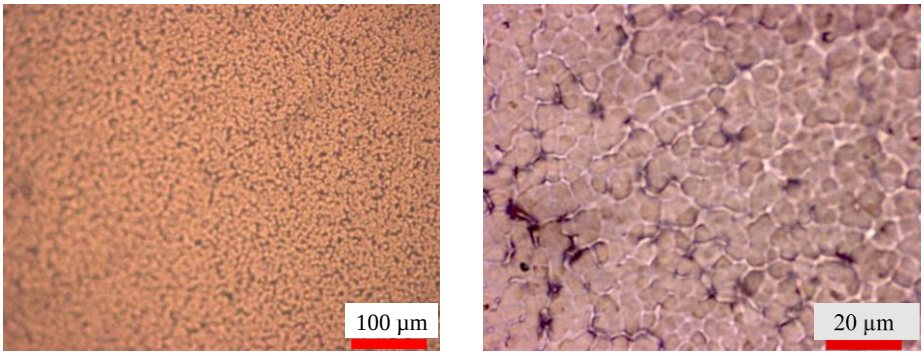

Figure 40: Optical images of pristine PVDF

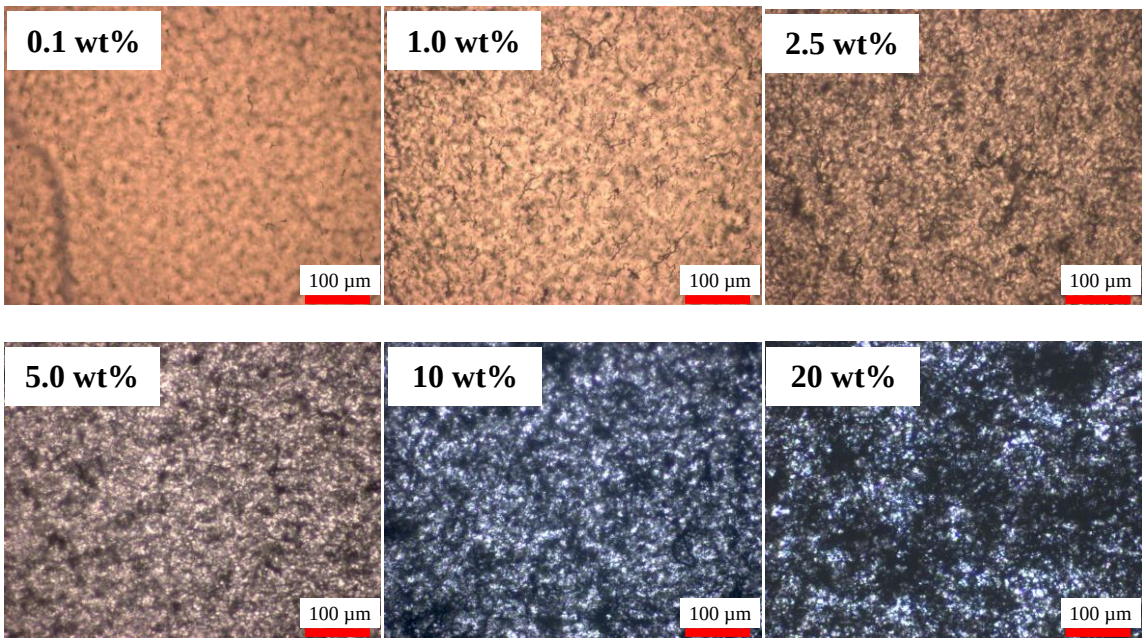

Figure 41: Optical images of PVDF films (x10 magnification)

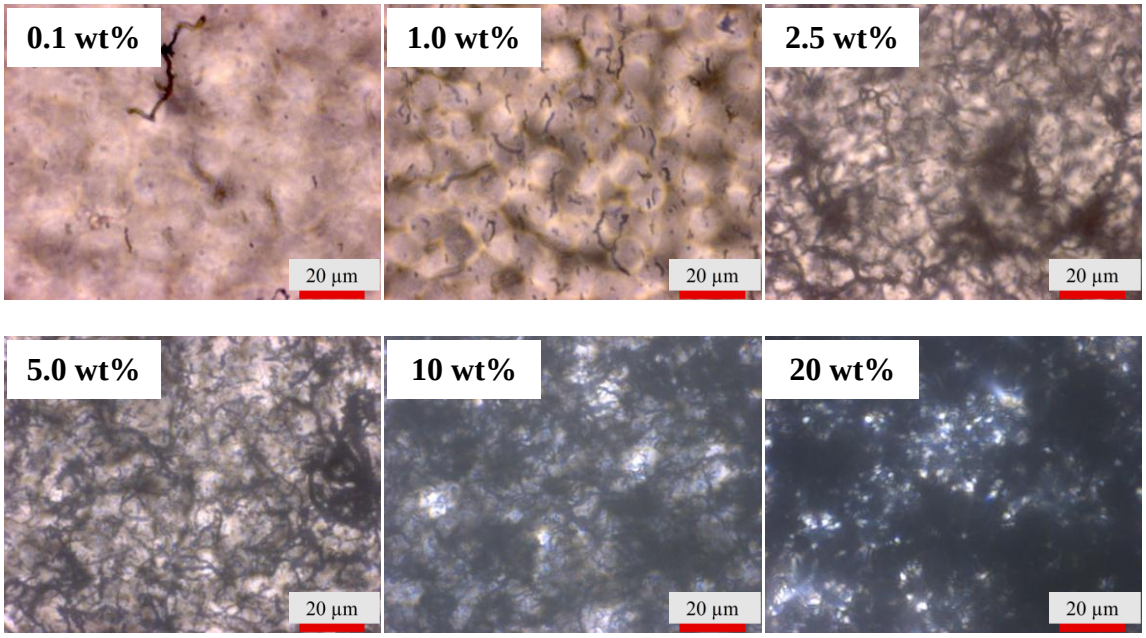

Figure 42: Optical images of PVDF films (x50 magnification)

The through thickness dispersion was observed to ensure that the NiNS did not settle during solidification. In order to better varify this thicker samples were made using the same molds used for epoxy. Due to solvent evaporation, the samples were not as thick as the epoxy samples and contained residual thermal stresses. Figure 43 and Figure 44 show the top layers, middle thirds and the bottom layer for a 0.1 wt% and 1.0 wt% nano-composite. Larger concentrations of NiNS in PVDF were not visible due to the saturation of particles blocking the light. It can be seen in both figures that NiNS are dispersed evenly throughout the thickness. Due to the high concentration it becomes more difficult to see the NiNS near the bottom layers especially in the

1.0 wt% sample but upon close inspection it is noted that the NiNS are present and dispersed.

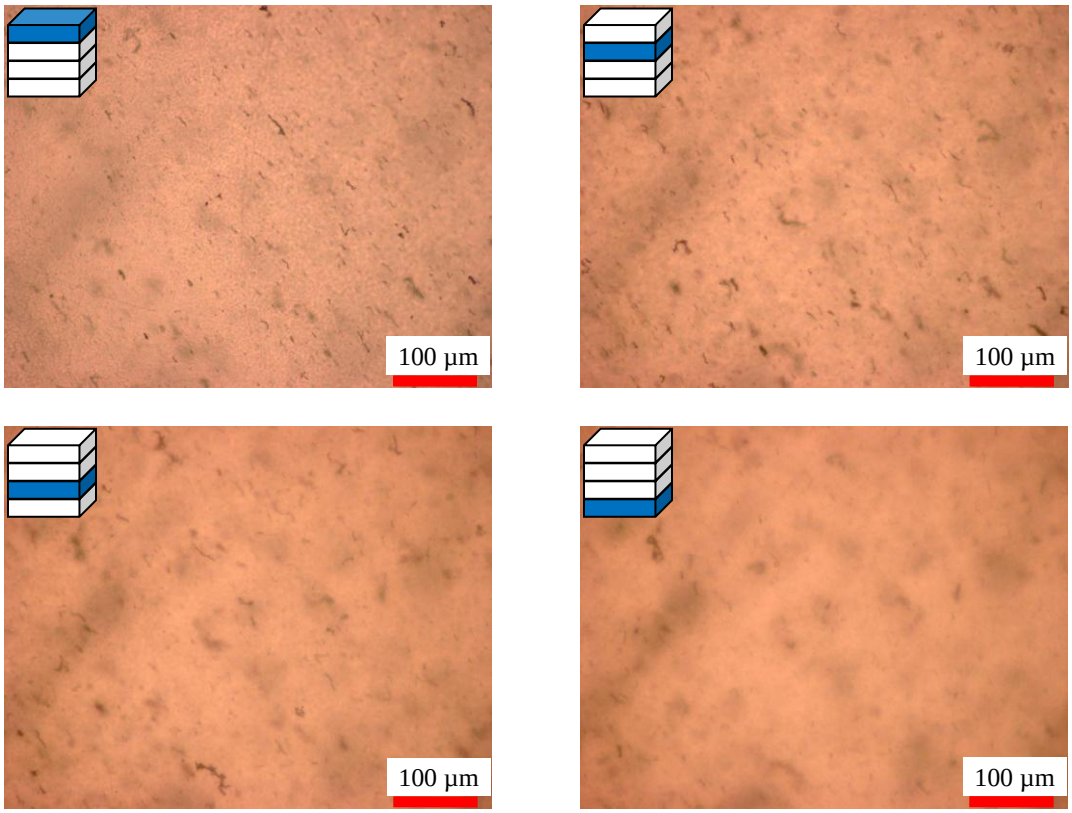

Figure 43: Optical images of 0.1 wt% NiNS - PVDF through thickness

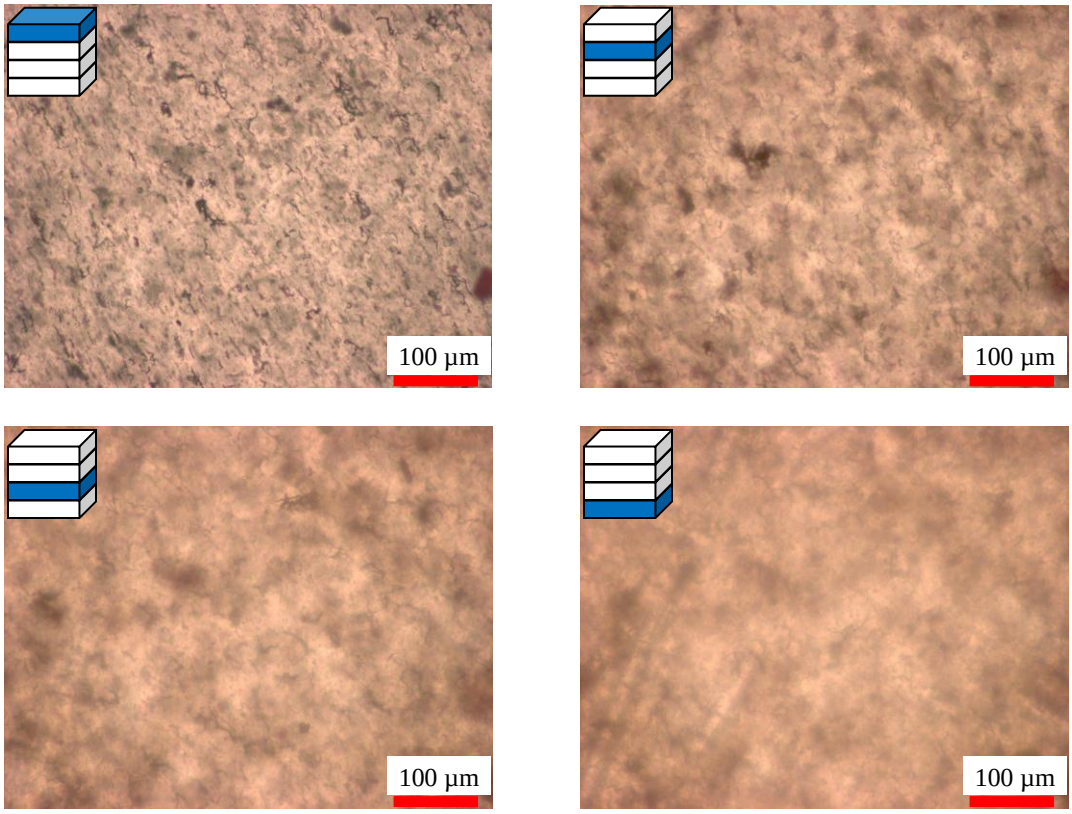

Figure 44: Optical images of 1 wt% NiNS - PVDF through thickness

The PVDF films were cut into strips and characterized using tensile testing. As stated for epoxy, each result is a representative sample picked from three or more samples. Figure 45 displays the storage modulus obtained for the PVDF values from a temperature range between -119°C to 90°C. Most noticeable from this data is the cross-over between the multiple samples near -50˚C.

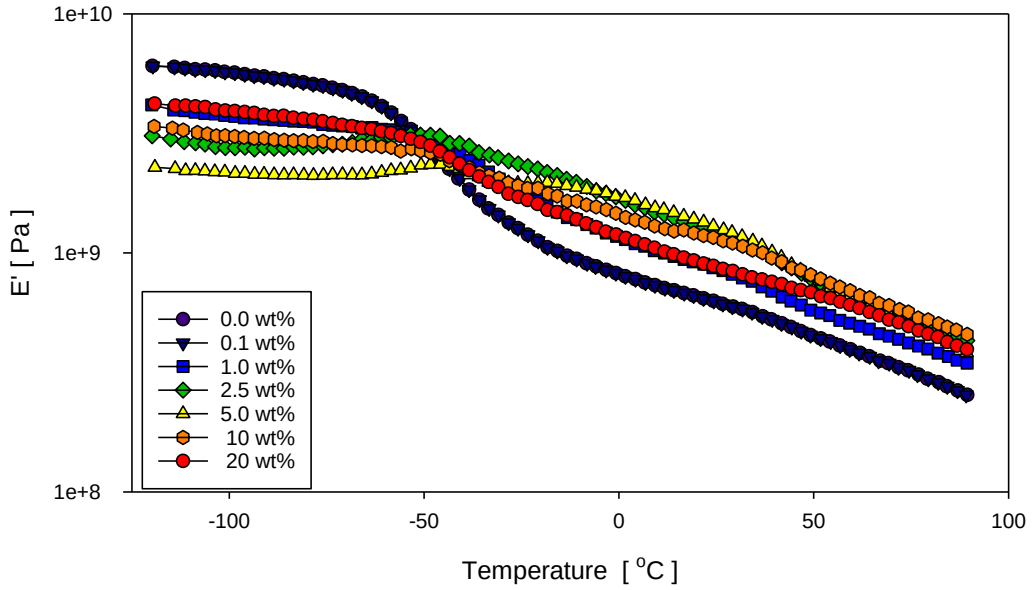

Figure 45: Storage Modulus

Before T_g, it is clearly seen that introducing NiNS causes a decrease in the storage modulus initially. Beyond 5 wt%, this trend reverses as the storage modulus increases with the 10 and 20 wt% samples although never overcoming the pristine sample. Figure 46 displays this trend at a temperature near -90°C. A decrease in the storage modulus occurs with the addition of NiNS until 5 wt% at which point the next sample, 10 wt%, and beyond display an increase but never fully reaches the storage modulus achieved by a pristine sample. Beyond the T_g, as can be seen in Figure 47 near a temperature of 50°C, the opposite trend is observed. The pristine sample has the lowest storage modulus that increases with the increase of NiNS. Above 5 wt%, the increase begins to steady with a slow increase and eventually decrease occurring en route to the 20 wt% sample.

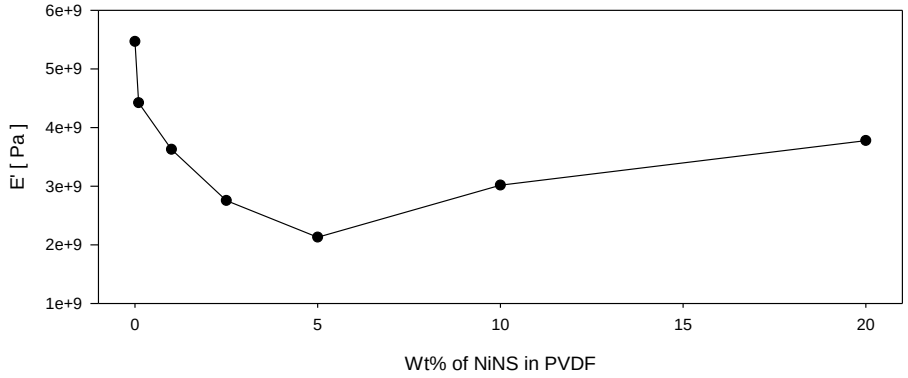

Figure 46: Storage Modulus near -90°C

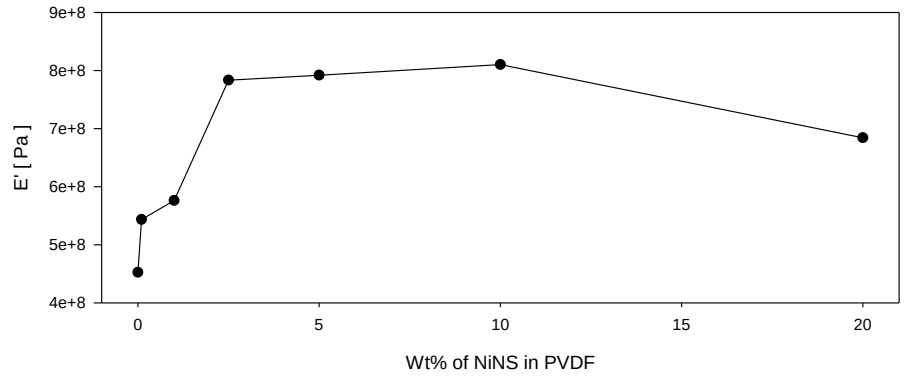

Figure 47: Storage Modulus near 50°C

The loss modulus measured for the PVDF is displayed in Figure 48 while Figure 49 and Figure 50 show the loss modulus at -90°C and 50°C respectively. The peaks observed in the loss modulus are commonly used to determine the T_g. Table 4 displays the measured T_g obtained by using this method. The introduction of NiNS is seen to increase the T_g up to 7.5°C. By observing the peak in the loss modulus, it can be determined that by introducing NiNS the T_g increases 5 to 7 °C and remains steady at that temperature. The measured

storage modulus at each peak is seen to be decreasing steadily from pristine to 20 wt% with only a few changes.

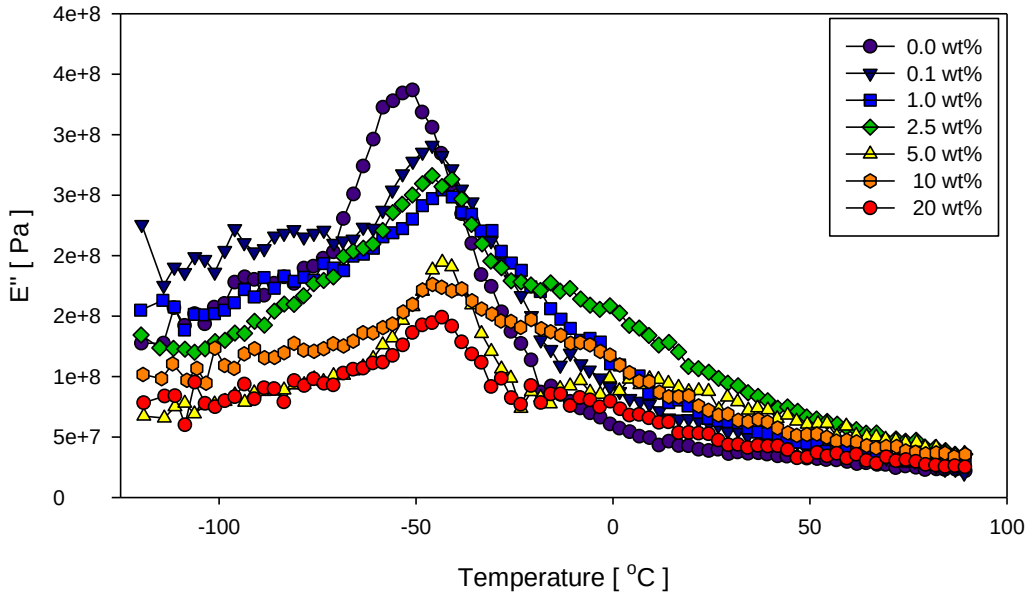

Figure 48: Loss Modulus

Table 4: T_g values obtained from DMA

	Peak Value (T_g) (°C)	Change (°C)
0.0 wt%	-50.91	0.00
0.1 wt%	-45.91	5.00
1.0 wt%	-43.38	7.53
2.5 wt%	-45.90	5.01
5.0 wt%	-43.32	7.59
10 wt%	-45.82	5.09
20 wt%	-43.43	7.48

Figure 49 displays the measured loss modulus near -90°C. A decrease in loss modulus can be observed until 5 wt% where a slight increase follows in the 10 wt% sample. The loss modulus once again decreases in value for the 20 wt% sample. At 50°C, an increase in loss modulus is observed until 2.5 wt% at which point a steady decrease is observed.

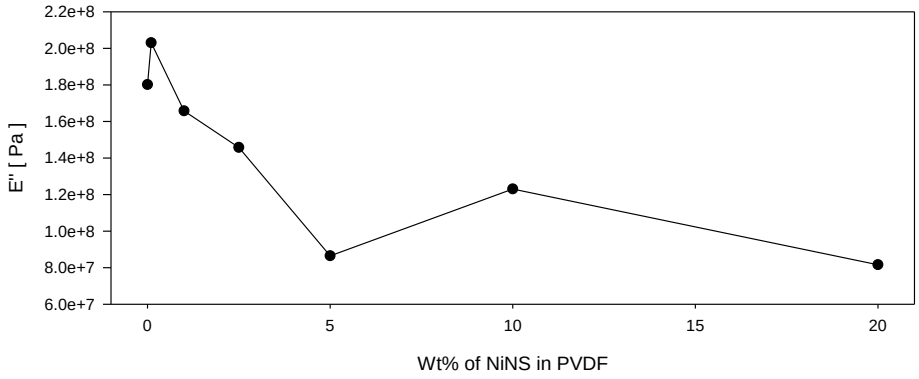

Figure 49: Loss Modulus near -90°C

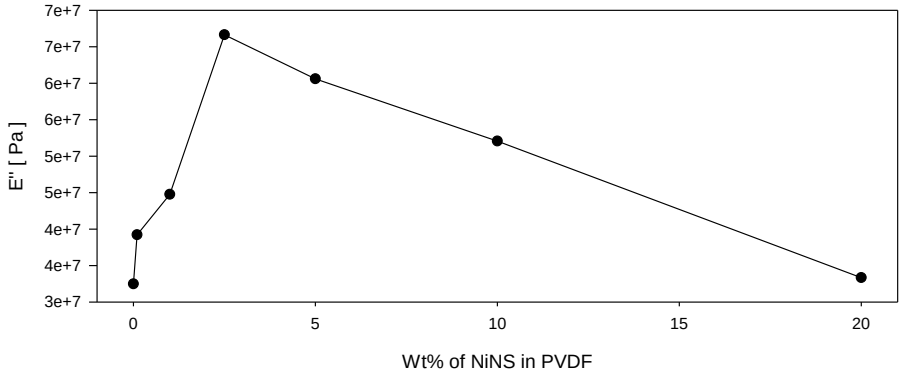

Figure 50: Loss Modulus near 50°C

The tan(δ) results shown in Figure 51 indicate that all the samples have a similar E’ to E’’ ratio throughout the temperature sweep and remain mostly

elastic. An increase in the tan(δ) values is observed with a small increase in NiNS concentration and begins to decrease with larger amounts before and after T_g. Figure 52 and Figure 53 show the results measured for tan(δ) near -90°C and 50°C respectively.

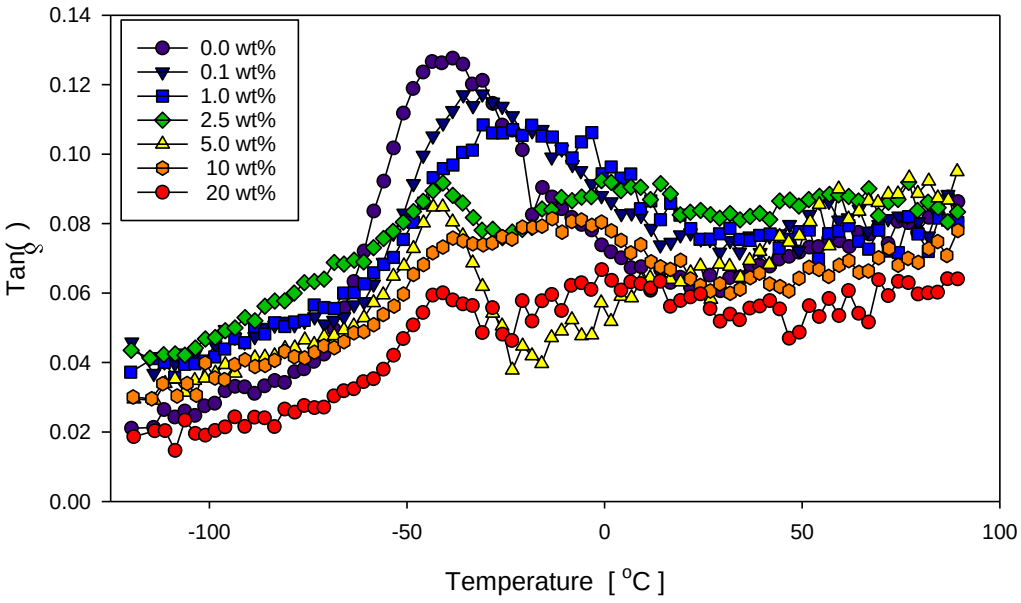

Figure 51: Tan(δ)

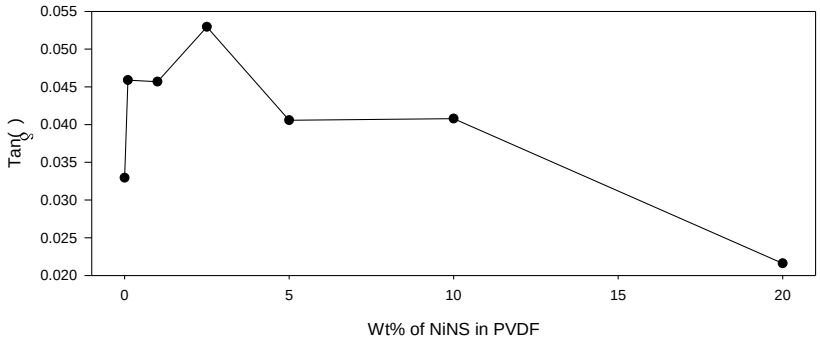

Figure 52: Tan(δ) near -90°C

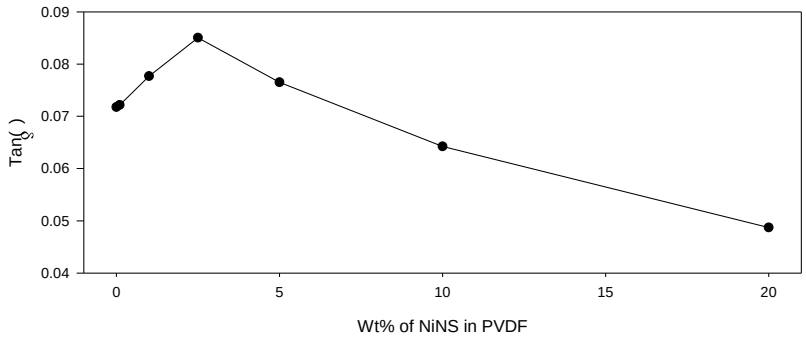

Figure 53: Tan(δ) near 50°C

By examining the PVDF films with a DSC, the percent crystallization as well as the melt temperature and crystallization temperature are measured and displayed in Table 5. The crystallization percentage was determined using instrument software and calculated using a consistent thermal range from 80°C to 200°C. Figure 54 displays the results from a DSC analysis performed on a 1 wt% NiNS – PVDF sample. Values are corrected by compensating for the NINS weight contribution. The adjusted percentage shows almost no change in crystallization up to 2.5 wt%. From 5.0 wt% onward, the percentage varies from -3 to 4 % indicating that a clear trend in the crystallization does not occur. Upon comparing the melt temperature, it can be seen that any addition of NiNS causes an increase in the melting temperature that is then tapered at 20 wt%. Crystallization temperature comparison shows that an increase in NiNS causes a decrease in the temperature. This indicates that the NiNS could be acting as a heterogeneous nucleation site and allows crystallization to occur at lower temperatures.

Table 5: DSC results for NiNS – PVDF

	V_{cry}	Adj V_{cry}	Δ Adj V_{cry}	T_m	Δ T_m	T_{cry}	Δ T_{cry}
0.0 wt%	53.6%	53.6%	0.0%	161.45	0.00	131.88	0.00
0.1 wt%	53.9%	54.0%	0.4%	162.70	1.25	130.31	-1.57
1.0 wt%	53.7%	54.2%	0.6%	168.00	6.55	130.15	-1.73
2.5 wt%	52.0%	53.3%	-0.3%	167.28	5.83	130.61	-1.27
5.0 wt%	48.0%	50.5%	-3.1%	165.42	3.97	129.88	-2.00
10 wt%	52.1%	57.8%	4.2%	166.09	4.64	128.27	-3.61
20 wt%	40.7%	50.9%	-2.7%	162.56	1.11	128.65	-3.23

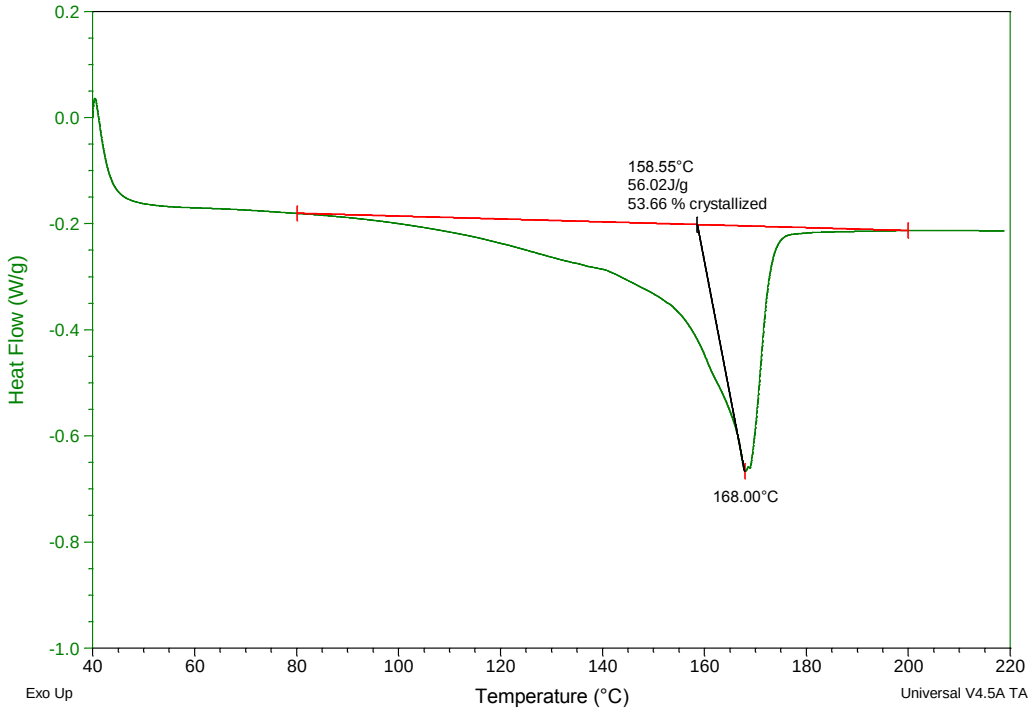

Figure 54: DSC analysis on 1 wt% NiNS – PVDF

When a film is characterized with FTIR, the percent reflectance is measured for various wavelengths. For PVDF the wavelengths of interest lay between 400 and 1500 cm^{-1}. At this wavelength, scale rotational-vibrational structures and more fundamental vibrations are observed. Using the peak

values measured for reflectance the PVDF films can be characterized in terms of their crystalline structure, namely if the PVDF structure is present in its alpha, beta or gamma phase. Peak values were obtained for each film and combined with the T_m of the samples obtained from DSC, the crystalline structure was classified. After comparison, it was determined that all the films contain a mixture of alpha and gamma phase and contain almost no beta phase segments. The addition of NiNS into the PVDF matrix, therefore, did not radically change the fundamental structure of the PVDF. Figure 55 displays the percent reflectance measurements for all films.

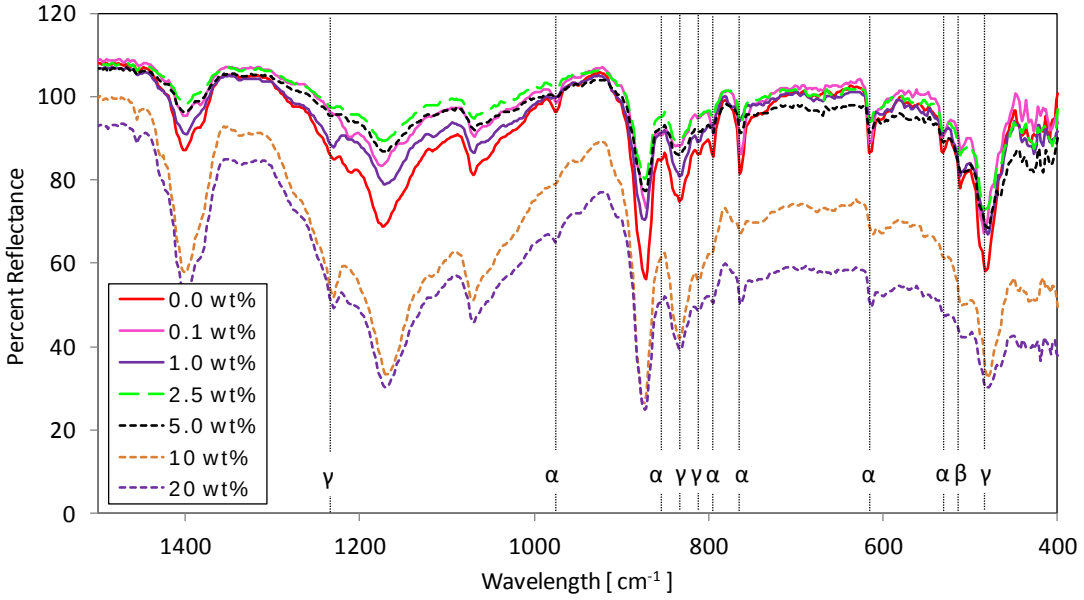

Figure 55: NiNS - PVDF FTIR Reflectance Results

Upon testing the electrical properties of the NiNS – PVDF nano-composites the 20 wt% displayed anomalous results and is not included in this analysis. At lower frequencies, the introduction of NiNS actually begins to decrease the dielectric constant up to 1.0 wt% NiNS concentration as can be seen in Figure 56. The dielectric constant increase at 2.5 wt% and continues onward passing the pristine sample at 10 wt%. At higher frequencies, as seen in Figure 57 which focuses at a frequency of 1.15 kHz, a small increase in NiNS in the composite results in a nearly negligible decrease in the dielectric constant but then begins to increase more drastically as it approaches 10 wt%.

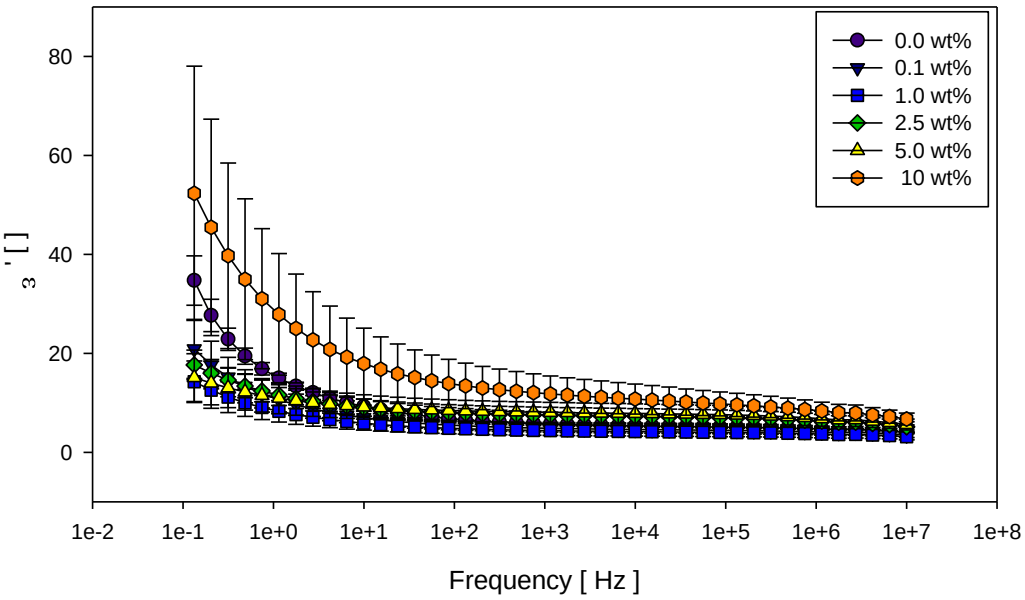

Figure 56: Dielectric constant at room temperature

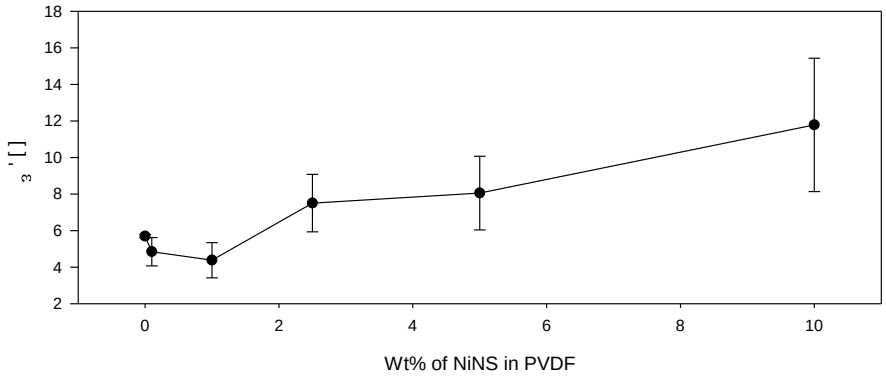

Figure 57: Dielectric constant at 1.15 kHz

By comparing the conductivity results in Figure 58 and Figure 59, it can clearly be seen that a decrease occurs all the way up to 5 wt%. At 10 wt%, an increase is finally observed. Again, the 20 wt% samples were too conductive causing a short in the system so it stands to reason that the percolation threshold for these films lie between 10 and 20 wt%.

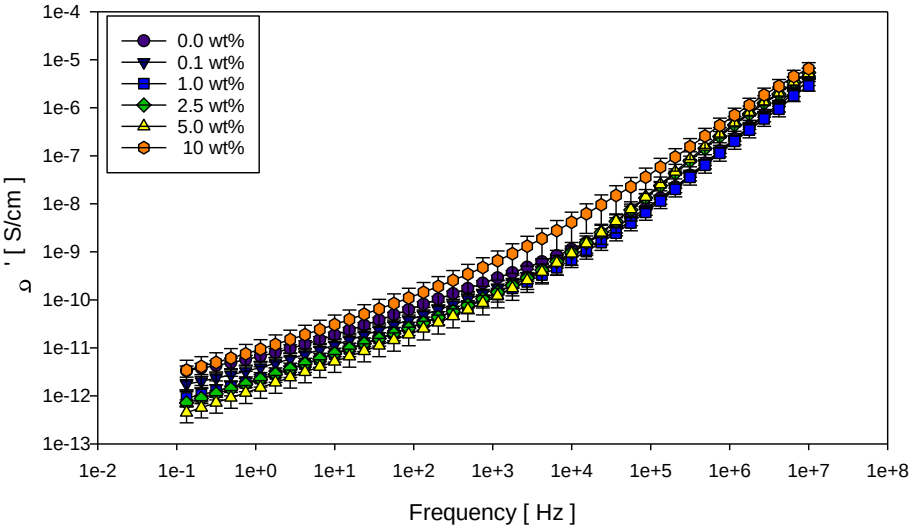

Figure 58: Conductivity

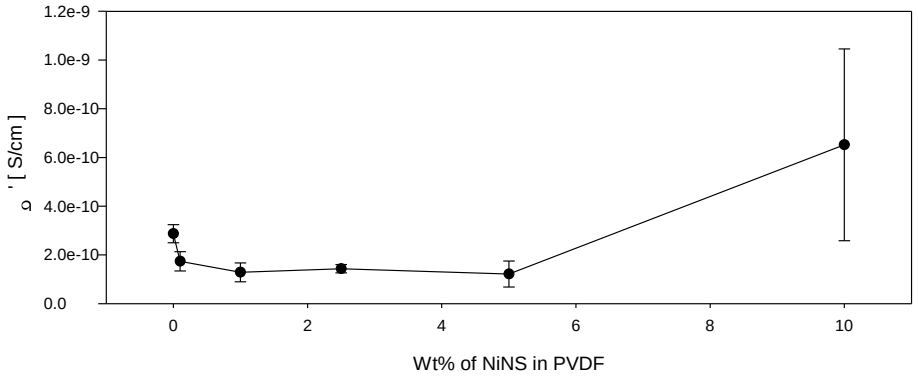

Figure 59: Conductivity at 1.15 kHz

The tan(δ) values in Figure 60 show that all samples generally behave identically in fashion. From Figure 61 it is more easily seen that with increasing NiNS wt% a decrease in the value of tan(δ) is observed until, once again, the 10 wt% sample.

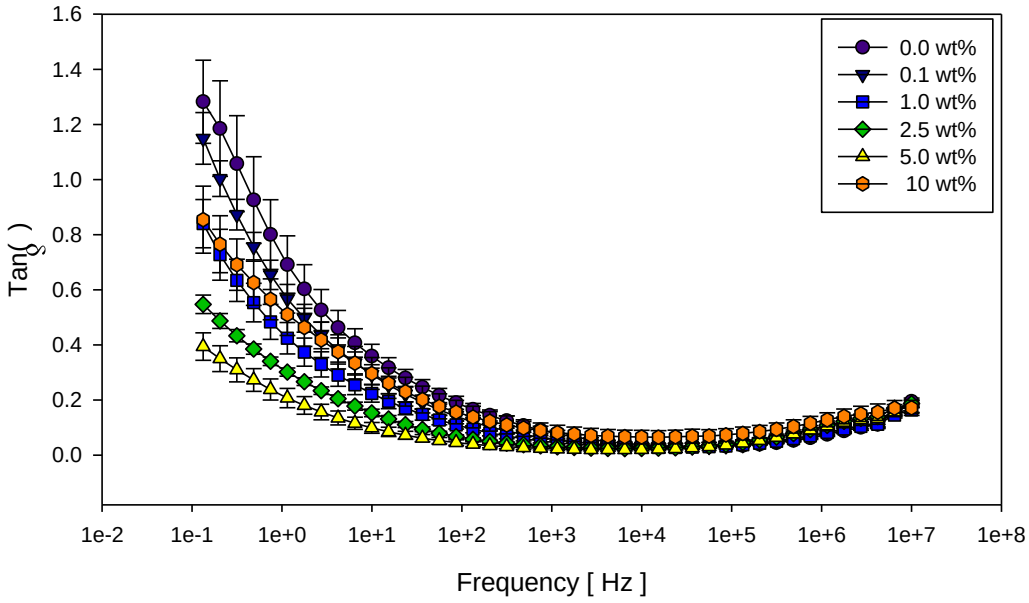

Figure 60: Tan(δ)

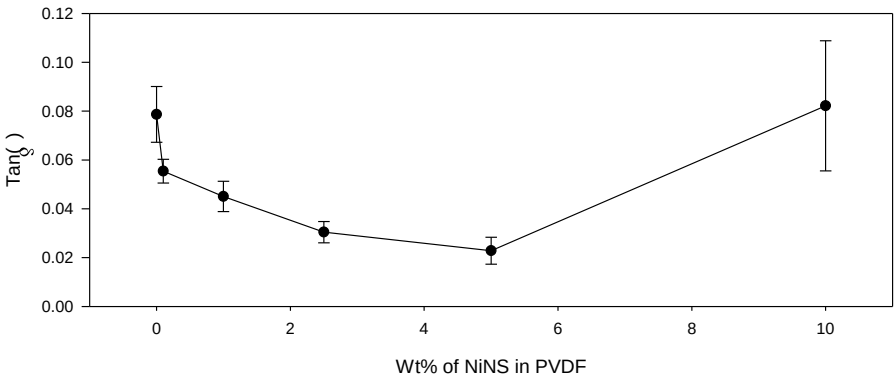

Figure 61: Tan(δ) at 1.15 kHz

3.6 PVDF nano-composite with PG solvent results

In another attempt to increase the dispersion of NiNS in the PVDF film, the solvent DMAc was exchanged for Propylene Glycol. Again, the NiNS were easily dispersed in the PG and showed good dispersion once added with the PVDF melt solution. The PG was then evaporated on a hot plate while undergoing continuous mixing. After some of the PG was evaporated, it was seen that the PVDF started to turn solid although it was above its melt temperature. In another attempt, the solution was poured into a mold before most of the PG was evaporated. PG was fully evaporated in the oven, it was observed that the PVDF had turned to white powder regardless of its high NiNS concentration. It was concluded that the PG had an adverse effect on the PVDF molecular chain and could not be used as a solvent for this polymer matrix.

CHAPTER IV

SUMMARY AND CONCLUSIONS

4.1 CP2 nano-composites

Initially CP2 was the polyimide of choice for dispersing NiNS in a thermoplastic polymer. A large factor in this decision stemmed from previous experience and success incorporating carbon nano-fibers into a nano-composite film using an in-situ polymerization technique developed for CP2. With in-situ processing it is expected that during the polymer chain growth stage the chains will wrap around the nano-sized particles effectively trapping and incorporating them into the matrix creating a well dispersed composite with well suspended particles. Although this process showed success with the CNFs near 100 nanometers in diameter, the same could not be confirmed for the larger sized NiNS that ranged from 50 nm to 2μm. While the smaller NiNS regions may have been successfully enveloped by the CP2, the bulk of the NiNS were too large and heavy to be suspended by the polyimide chains for an extended amount of time.

The processing technique used for the CP2 resulted in a well-dispersed solution that could have adjustable viscosity depending on the amount of solvent present. In early attempts at NiNS nano-composites, a large amount of focus was dedicated to overcoming agglomerations and two-phase composites. After many attempts and variations, a seemingly well dispersed film was processed using the technique described previously. After several films were produced and

characterized, it was determined that the NiNS settled to the bottom of the film during the lengthened cure time. It became apparent that the in-situ polymerization of CP2 was not able to suspend the heavy NiNS and any positive effect that was experienced from the in-situ polymerization was counteracted during the cure cycle due to the matrix's low viscosity at high temperatures for extended times. From the characterization results, it was determined that in order for CP2 to be a viable polymer, large modifications would need to be implemented. Some possibilities include changing the solvent for one that has a more stable interaction with the NiNS and does not detrimentally affect the matrix or that the NiNS must all have a smaller diameter that allows for encapsulation during the in-situ polymerization. It would appear from these results that maintaining a dispersed NiNS nano-composite reliant only on the principles of in-situ processing is not possible.

4.2 Epoxy nano-composites

The initial procedure for creating an epoxy nano-composite with fillers was also obtained from prior success in creating CNF composites. This method did not work as well, however, due to the ineffectiveness of the solvent DMAc to suspend the nano-particles for any lengthened time even when mixed with the resin as was observed during the attempted degassing stages. The only solvent that was more effective than the DMAc, PG, unfortunately appeared to react chemically with the epoxy. Unable to find a solvent capable of suspending the

NiNS while maintaining a positive interaction with the epoxy matrix, it became necessary to bypass the solvent phase by directly adding the NiNS particles to the resin. Foregoing the solvent also meant losing the aid of the probe sonicator and having to use the bath sonicator as the primary nano-scale dispersion instrument.

A procedure was quickly determined which allowed for good dispersion and the removal of large agglomerates without the aid of solvents. Once this well-mixed solution was poured into a mold it became clear that this composite was also suffering from NiNS settling throughout the film. Although the epoxy is a thermoset, which begins to harden once sufficient curing has been established, the solution has a drastic decrease in viscosity at the high temperatures before adequate hardening can occur. It is during these elevated temperatures that the NiNS begin to settle establishing a two-phase composite. In an effort to combat this decreased viscosity, the solution was allowed to mix for an elevated temperature and time allowing the curing agent and resin to begin hardening. The initial two hours at 125°C was also bypassed due to this lengthened mixing time. While the mixture is harder to handle with the severely increased viscosity, it is the author's belief that proper industrial equipment and heating will allow for simpler application of the composite. Once heated to its final cure temperature the mixture decreases slightly in viscosity allowing the composite mixture to spread throughout the mold and creates a smooth top

layer. A very small amount of NiNS settling does appear to occur during this stage but the particle free top layer is easily removed with sanding or polishing.

After observing the unpolished samples with the OM and characterizing the polished samples, it was determined that this process leads to a generally uniform and dispersed nano-composite. With increasing wt% of NiNS, it can be seen that an increase in the electrical conductivity and dielectric constant occurs. Beyond the composites T_g, all electrical properties increase in value. The glass transition temperature does not appear to be influenced by the NiNS concentration when tested with the DSC. An increase in the storage modulus can also be observed when the composite is past its T_g indicating interaction between the NiNS and the epoxy polymer chains. This method provided a novel processing technique to successfully disperse NiNS in an Epon 862 resin epoxy. The driving force behind this success relies on the high viscosities obtained and the relative quickness to hardening once mixing is stopped. Viscosity increases in this epoxy system to due to the onset of crosslinking when the hardening agent is added. This crosslinking, not only leads to a polymer mixture that becomes increasingly more difficult to move over time but it also restricts movement of the NiNS particles significantly. However, during the final heat cure of the epoxy, the viscosity again begins to decrease. This does allow for the epoxy to take the shape of the mold but also allows for easier NiNS movement. Due to this, it is also necessary for the epoxy to harden quickly to restrain the NiNS from settling further. If high viscosity after mixing and a quick cure can be

achieved, a well-dispersed NiNS nano-composite can be achieved for similar thermosets.

4.3 PVDF nano-composites

In another attempt to successfully disperse NiNS in a thermoplastic polymer, a melt solution technique was developed and used. Solvent was used primarily to break up NiNS agglomerates and disperse the particles throughout a PVDF solution. Once dispersion has been achieved, the solvent was evaporated while simultaneously melting the PVDF. Once most of the solvent had been removed, the melt solution was poured into a mold or spread into a film. The melt solution was then placed in an oven at a temperature that would quickly, but not violently, remove the remaining solvent while also quickly cooling the PVDF into a solid. This method, much like the epoxy method, primarily traps NiNS into a dispersed state by quickly hardening in a high viscosity state rather than rely on solvent-particle or polymer-particle interaction.

This technique led to polymer nano-composites that were well dispersed when observed with the OM. By observing the storage modulus, an interesting result can be observed. Below the T_g of the PVDF, a decrease in the storage modulus occurs as NiNS concentration increases up to 5 wt%. Beyond 5 wt%, the storage modulus begins to increase but never achieves the pristine PVDF values. Above the T_g, the reverse trend is observed with the 5 wt% nano-composite being among the highest value. Viewing these two factors together

could imply that there are strong NiNS – PVDF interaction above T_g but a more detrimental interaction when the PVDF chains are more brittle. A similar pattern can be observed with the loss modulus where trends reverse below and above T_g. The T_g of the films themselves were obtained using the loss modulus and indicated a slight increase in the T_g with the addition of NiNS.

DSC results showed a decrease in crystallization temperature with an increased NiNS concentration while the percent crystallization and melt temperature increased for some of the contents then mostly decreased again. FTIR characterization indicated that the films contain alpha and gamma phases and type of crystallinity does not change dramatically with NiNS presence. The electrical results obtained from dielectric spectroscopy were very different than was expected. With a small increase in NiNS, the values for the dielectric constant and conductivity dropped at lower frequencies. After a certain concentration of NiNS was passed both values started to increase .At higher frequencies the dielectric constant and conductivity increased at a much lower NiNS concentration. At lower frequencies, the PVDF matrix plays a larger role concerning electrical properties, which becomes hindered with small additions of NiNS. At higher frequencies the values are determined more so by the NiNS concentration. As can be seen by Figure 58, somewhere between 5 and 10 wt%, a switch is made where frequency is no longer a driving factor, but rather an increase in the concentration of NiNS directly increases the electrical properties at any frequency. By increasing the NiNS concentration, the particles begin to

create a conductive network, which becomes a bigger factor in determining the dielectric constant and conductivity. Eventually, and most likely soon after 10 wt%, the NiNS network becomes fully conductive.

After examining the optical images and the characterization results, it is found that a successfully dispersed NiNS – thermoplastic nano-composite was processed. The characterization results provided interesting data concerning the mechanical and electrical properties. Although these results are interesting in their own aspect, they all point to a well dispersed nano-composite. Similar to the previously stated requirements for well dispersed thermoset composites, this thermoplastic composite was possible due to the viscosity of the mixture before casting and the rapid hardening of the matrix below the melting temperature. In this case, the majority of the solvent used had evaporated causing the PVDF to become more viscous, although not nearly as viscous as the epoxy was. Upon exposure to temperatures below the melt temperature, the PVDF quickly gelled, as the remaining solvent was not sufficient to dissolve the polymer chains completely. This gelling was accompanied by a quick increase in viscosity that appeared to hold the NiNS firmly in place. By keeping the temperature elevated, the remaining solvent slowly evaporated until only the NiNS – PVDF nano-composite remained. This procedure should be easily repeatable for any thermoplastics under two conditions: 1) The solvent does not violently boil near the thermoplastic's melt temperature and 2) the solvent can reasonably evaporate below the polymer's melt temperature.

4.4 Final conclusions and summary

Throughout this thesis, three different polymers were used in the attempt to create a NiNS – polymer nano-composite. The objective was to create well dispersed composites with each of these polymers and then characterize some basic mechanical, thermal, electrical and dialectical properties. The first polymer experimented with was CP2. This thermoplastic polyimide allowed for in-situ processing in an attempt to entangle the polymer chains around the particles. This process was unable to generate a dispersed NiNS composite however due to the inability for the polymer chains to support the NiNS during the cure cycle. Testing with this polymer identified future problems that may be encountered, most importantly, the settling of NiNS during non-mixing stages.

The second polymer pursued was an Epon 862, an epoxy. This polymer differed primarily from the CP2 in that it is a thermoset, which means the epoxy will harden during the cure cycle. After several techniques were attempted, a successful process was created which primarily used viscosity as a means to create a well dispersed nano-composite. The epoxy would slowly begin to thicken during a low temperature cure phase in which the NiNS were continuously being mixed. With a high viscosity and being partially cured, the mixture was cast and finished curing quickly. This method relies on physically hindering the settling of the particles. The third polymer tested was thermoplastic PVDF. The method used to successfully disperse NiNS in this polymer relied on the rapid hardening that can be achieved when a polymer is cooled below its

melt temperature. The NiNS particles were first dispersed in a solvent and then in the PVDF as a solution. The solution was heated to remove most of the solvent and melt the polymer at which point it was cooled below T_m. At this temperature, the PVDF hardened, again physically trapping the NiNS, while the remaining solvent evaporated. This method, much like the epoxy, relied on physically trapping the particles in a dispersed state quickly.

The epoxy and PVDF both demonstrated an increase in the storage modulus when tested beyond their respective T_g. Below T_g the epoxy showed only a slight increase while the PVDF composite showed a dramatic decrease. In both composites, the measured T_g was not greatly altered by an increase in NiNS particles. Both polymers required samples beyond 10 wt% to achieve the percolation threshold with regards to electrical properties. The epoxy samples showed a consistent increase in conductivity and dielectric constant while the PVDF first underwent a decrease before an increase was observed. Addition of NiNS to the PVDF composite did not result in a fundamental change in the crystallinity when examined with FTIR.

Looking at the 10 wt% results, this concentration can be restated as 1.4 vol% for an epoxy sample and 2.16 vol% for a PVDF sample. Relating this vol% to the amount of SWNTs required to reach the percolation threshold in epoxy for example, approx. 0.78 vol%, as measured by Sumanth, et al shows that NiNS may require more than twice the volume to achieve percolation [6]. To compare cost effectiveness of these samples, consider a 100g epoxy sample. To reach

near the percolation threshold for SWNTs, 1.5g will be used, equaling near $300 in today's prices. For NiNS, consider a 20 wt% sample that may be closer or above the percolation threshold using the PVDF results as a basis. This 20 wt% NiNS – epoxy composite will require 20g of NiNS costing near $100. Clearly, the cost differences may be a major factor when determining a nano-particle with which to reinforce a polymer. The downside with this choice, however, is the large volume occupied by the particles as well as the weight addition and any mechanical effects that could occur. Combining these two factors leads to a conclusion that NiNS may be better suited then SWNTs strictly depending on the application and comparing only electrical properties. Furthermore, NiNS also provide additional properties that such as magnetism that could be used to create composites that interact with magnetic fields or possibly enhanced interaction when fused with other metal surfaces.

This research attempted several processing methods to obtain a dispersed NiNS nano-composite. It showed that common nano-composite processing techniques such as solvent casting and in-situ polymerization do not work well with NiNS, rather high viscosity and a quick solidification time is key. This work is a first attempt to explore dispersion and processing of NiNS nano-composites. By observing several characteristic properties of these nano-composites, it was also shown that the addition of a small quantity of NiNS can greatly affect mechanical properties and, although a larger vol% may be required, electrical conductivity can be achieved for a much lower price. For

further research with NiNS in polymer composites, the percolation threshold still needs to be determined. Some possible technique alterations that could enhance the dispersion and characterization results include the use of non-violent means to break up NiNS agglomerates and create a good dispersion. The use of a better solvent or surfactant should also be examined.

References

1. Ghaseminejhad, M. & A. Parvizi-Majidi, Impact behaviour and damage tolerance of woven carbon fibre-reinforced thermoplastic composites. *Construction and Building Materials* **4**, 194-207 (1990).
2. Bao, L.R. & A.F. Yee, Effect of temperature on moisture absorption in a bismaleimide resin and its carbon fiber composites. *Polymer* **43**, 3987-3997 (2002).
3. Cantwell, W., P. Curtis, & J. Morton, Post-impact fatigue performance of carbon fibre laminates with non-woven and mixed-woven layers. *Composites* **14**, 301-305 (1983).
4. Salehi-Khojin, A., Mahifalah, M. Bashirzadeh, R.& Freeman, B., Temperature effects on Kevlar/hybrid and carbon fiber composite sandwiches under impact loading. *Composite Structures* **78**, 197-206 (2007).
5. Lan-Hui, S., Ounaies, Z., Gao, X., Whalen, C., & Yang, Z., Preparation, Characterization, and Modeling of Carbon Nanofiber/Epoxy Nanocomposites. *Journal of Nanomaterials vol.* **2011**, 75-82 (2011).
6. Banda, S., Electric field manipulation of polymer nanocomposites: Processing and investigation of their physical characteristics. Doctoral dissertation, Texas A&M University (2008).
7. Deshmukh, S., Effect of single walled carbon nanotubes (SWNTs) on the electromechanical properties of polyimide nanocomposites, Master's Thesis, Texas A&M University (2006).
8. Deshmukh, S. & Ounaies, Z. Single walled carbon nanotube (SWNT)-polyimide nanocomposites as electrostrictive materials. *Sensors and Actuators A: Physical* **155**, 246-252 (2009).
9. Khodaparast, P. & Ounaies, Z. Preparation of TiO Polymer Nanodielectrics via a Solvent-Based Technique. *ASME Conf. Proc.* 2010, 239 (2010).

10. Lu, H., Gou, J., Leng, J., & Du, S., Synergistic effect of carbon nanofiber and sub-micro filamentary nickel nanostrand on the shape memory polymer nanocomposite. *Smart Materials and Structures* **20**, 035017 (2011).
11. Ghose, S., Watson, K. A., Working, D.C., Connell, J.W., Smith, Jr, J.G., Lin, Y., & Sun, Y.P., Thermal Conductivity of Copoly(ethylene vinyl acetate)/Nano-filler Blends, SAMPE 2007 Symposium and Exhibition - Baltimore, MD, (2007).
12. Biercuk, M., Liaguno, M., Radosavljevic, M., Hyun, J., Johnson, A., et al., Carbon nanotube composites for thermal management. *Applied Physics Letters* **80**, 2767 (2002).
13. Chakravarthi, D.K., Khabashesku, V., Vaidyanathan, R., Blaine, J., Yarlagadda, S., et al., Carbon Fiber–Bismaleimide Composites Filled with Nickel Coated Single Walled Carbon Nanotubes for Lightning Strike Protection. *Advanced Functional Materials* **21**, 2527-2533 (2011).
14. Mackay, M., Tuteja, A., Duxbury, P., Hawker, C., Horn, B., et al., General strategies for nanoparticle dispersion. *Science* **311**, 1740 (2006).
15. Liu, W., Tian, X., Cui, P., Li, Y., Zheng, K., et al., Preparation and characterization of PET/silica nanocomposites*. Journal of Applied Polymer Science* **91**, 1229-1232 (2004).
16. Lee, C.S., J.S. Lee, & S.T. Oh, Dispersion control of Fe2O3 nanoparticles using a mixed type of mechanical and ultrasonic milling. *Materials Letters* **57**, 2643-2646 (2003).
17. Inkyo, M. & T. Tahara, Dispersion of agglomerated nanoparticles by fine beads mill. *J. Soc. Powder Technol* **41**, 578–585 (2004).
18. Pegel, S., Potschke, P., Petzold, G., Alig, I., Dudkin, S., et al., Dispersion, agglomeration, and network formation of multiwalled carbon nanotubes in polycarbonate melts*. Polymer* **49**, 974-984 (2008).

19. Tseng, W.J. & S.Y. Lin, Effect of polymeric surfactant on flow behaviors of nickel-ethanol-isopropanol suspensions. *Materials Science and Engineering A* **362**, 160-166 (2003).
20. Li, Y., Li, C., Wang, H., Li, L., & Qian, Y., Preparation of nickel ultrafine powder and crystalline film by chemical control reduction. *Materials Chemistry and Physics* **59**, 88-90 (1999).
21. Moore, V.C., Strano, M., Haroz, E., Hauge, R., Smalley, R., et al., Individually suspended single-walled carbon nanotubes in various surfactants. *Nano Letters* **3**, 1379-1382 (2003).
22. Matarredona, O., Rhoads, H., Li, Z., Harwell, J., Balzano, L., et al., Dispersion of single-walled carbon nanotubes in aqueous solutions of the anionic surfactant NaDDBS. *The Journal of Physical Chemistry B* **107**, 13357-13367 (2003).
23. Vaisman, L., H.D. Wagner, & G. Marom, The role of surfactants in dispersion of carbon nanotubes. *Advances in Colloid and Interface Science* **128**, 37-46 (2006).
24. Dyke, C.A. & M. James, Unbundled and highly functionalized carbon nanotubes from aqueous reactions. *Nano Letters* **3**, 1215-1218 (2003).
25. Dyke, C.A. & M. James, Solvent-free functionalization of carbon nanotubes. *Journal of the American Chemical Society* **125**, 1156-1157 (2003).
26. Mitchell, C., Bahr, J., Arepalli, S., Tour, J., & Krishnamoorti, R., Dispersion of functionalized carbon nanotubes in polystyrene. *Macromolecules* **35**, 8825-8830 (2002).
27. Duncan, N.A., Changes to Electrical Conductivity in Irradiated Carbon Nanocomposites, Master's Thesis, Air Force Institue of Technology Wright-Patterson AFB. (2011).

28. Gou, J., Tang, Y., Liang, F., Zhao, Z., Firsich, D., et al., Carbon nanofiber paper for lightning strike protection of composite materials. *Composites Part B: Engineering* **41**, 192-198 (2010).
29. Ghose, S., Watson, K., Working, D., Connell, J., Smith, J., et al., Thermal conductivity of ethylene vinyl acetate copolymer/nanofiller blends. *Composites Science and Technology* **68**, 1843-1853 (2008).
30. McGary, J.D., Electrostatic Discharge Properties of Irradiated Nanocomposites, Master's Thesis, Air Force Institue of Technology Wright-Patterson AFB (2009).
31. Whitworth, D., Miles, M., Fullwood, D., Hansen, G., & Strong, B., Electrical Properties Of Polyethylene With Nickel Nanostrands And Nickel Coated Carbon Fiber Reinforcement, *SAMPE Conf. Proc.* 42nd ISTC - Salt Lake City (2010).
32. Whitworth, D.A., Processing a Nickel Nanostrand and Nickel Coated Carbon Fiber Filled Conductive Polyethylene by Injection Molding, Master's Thesis, Brigham Young University (2010).
33. Lanceros-Mendez, S., Mano, J., Costa, A., & Schmidt, V., FTIR and DSC studies of mechanically deformed β-PVDF films*. Journal of Macromolecular Science. Physics* **40**, 517-527 (2001).

VITA

Name: Casey Allen Whalen

Address: 701 H.R. Bright Building
Aerospace Engineering Department
College Station Tx, 77843

Email Address: casey_whalen@tamu.edu

Education: B.A., Aerospace Engineering, Texas A&M University, 2009
Math Minor; Polymer Specialty Certificate
GPA: 3.177
M.S., Aerospace Engineering, Texas A&M University, 2011
Advisor: Dr. Zoubeida Ounaies
GPA: 3.227

Research Experience:

Texas A&M University
Electroactive Materials Characterization Lab (Jan 2007 – Oct 2011)
Advisor: Dr. Zoubeida Ounaies

- Fabricated and characterized nano-composites consisting of Carbon Nanotubes, Nickel Nanostrands or Nanoclays in polymer matrices.

Publications:

- Lan-Hui, S., et al., *Preparation, Characterization, and Modeling of Carbon Nanofiber/Epoxy Nanocomposites. Journal of Nanomaterials, 2010.*
- Whalen, C. and Z. Ounaies, *Dispersion and Characterization of Nickel Nanostrands in Thermoset and Thermoplastic Polymers. (Masters Dissertation. Soon to be published)*